Original article

Selenium nanoparticles from *Lactobacillus paracasei* HM1 capable of antagonizing animal pathogenic fungi as a new source from human breast milk

Mohamed T. El-Saadony [a], Ahmed M. Saad [b], Taha F. Taha [b], Azhar A. Najjar [c], Nidal M. Zabermawi [c], Maha M. Nader [a], Synan F. AbuQamar [d,*], Khaled A. El-Tarabily [d,e,*], Ali Salama [a]

[a] *Department of Agricultural Microbiology, Faculty of Agriculture, Zagazig University, Zagazig 44511, Egypt*
[b] *Biochemistry Department, Faculty of Agriculture, Zagazig University, Zagazig 44511, Egypt*
[c] *Department of Biological Sciences, Faculty of Science, King Abdulaziz University, Jeddah 21589, Saudi Arabia*
[d] *Department of Biology, College of Science, United Arab Emirates University, 15551 Al-Ain, United Arab Emirates*
[e] *Harry Butler Institute, Murdoch University, Murdoch 6150, Western Australia, Australia*

ARTICLE INFO

ABSTRACT

The current study was performed to develop a simple, safe, and cost-effective technique for the biosynthesis of selenium nanoparticles (SeNPs) from lactic acid bacteria (LAB) isolated from human breast milk with antifungal activity against animal pathogenic fungi. The LAB was selected based on their speed of transforming sodium selenite (Na_2SeO_3) to SeNPs. Out of the four identified LAB isolates, only one strain produced dark red color within 32 h of incubation, indicating that this isolate was the fastest in transforming Na_2SeO_3 to SeNPs; and was chosen for the biosynthesis of LAB-SeNPs. The superior isolate was further identified as *Lactobacillus paracasei* HM1 (MW390875) based on matrix-assisted laser desorption ionization-time of flight mass spectrometry (MALDI-TOF MS) and phylogenetic tree analysis of 16S rRNA sequence alignments. The optimum experimental conditions for the biosynthesis of SeNPs by *L. paracasei* HM1 were found to be pH (6.0), temperature (35C), Na_2SeO_3 (4.0 mM), reaction time (32 h), and agitation speed (160 rpm). The ultraviolet absorbance of *L. paracasei*-SeNPs was detected at 300 nm, and the transmission electron microscopy (TEM) captured a diameter range between 3.0 and 50.0 nm. The energy-dispersive X-ray spectroscopy (EDX) and the Fourier-transform infrared spectroscopy (FTIR) provided a clear image of the active groups associated with the stability of *L. paracasei*-SeNPs. The size of *L. paracasei*-SeNPs using dynamic light scattering technique was 56.91 ± 1.8 nm, and zeta potential value was −20.1 ± 0.6 mV in one peak. The data also revealed that *L. paracasei*-SeNPs effectively inhibited the growth of *Candida* and *Fusarium* species, and this was further confirmed by scanning electron microscopy (SEM). The current study concluded that the SeNPs obtained from *L. paracasei* HM1 could be used to prepare biological antifungal formulations effective against major animal pathogenic fungi. The antifungal activity of the biologically synthesized SeNPs using *L. paracasei* HM1 outperforms the chemically produced SeNPs. *In vivo* studies showing the antagonistic effect of SeNPs on pathogenic fungi are underway to demonstrate the potential of a therapeutic agent to treat animals against major infectious fungal diseases.

* Corresponding authors at: Department of Biology, College of Science, United Arab Emirates University, 15551, Al-Ain, United Arab Emirates (S.F. AbuQamar and K.A. El-Tarabily).

E-mail addresses: sabuqamar@uaeu.ac.ae (S.F. AbuQamar), ktarabily@uaeu.ac.ae (K.A. El-Tarabily).

1. Introduction

Fungi are an extremely versatile class of organisms which can attack different hosts, causing many serious diseases (Seyedmousavi et al., 2018). The importance of fungal infections in humans and animals has increased over the last two decades (Dworecka-Kaszak et al., 2020). These diseases caused by fungi can be difficult to treat due to developing resistance to standard antifungal drugs (Fisher et al., 2012; Yapar, 2014).

The filamentous fungus *Fusarium* and the yeast *Candida* infects animals and causes several diseases. The genus *Candida* includes>200 species, of which 15 have been identified as the causal agents of many human and animal diseases (Yapar, 2014). The most prominent of these pathogens are *Candida albicans, C. glabrata, C. krusei, C. parapsilosis* and *C. tropicalis*. Diseases associated with *C. albicans* and *C. glabrata* often occur in warm-blooded hosts (Yapar, 2014). *Candida* infection usually occurs by the colonization of the host rather than the longitudinal and vertical transmission (Yapar, 2014).

Fusarium is one of the emerging causes of opportunistic mycoses, with approximately 15 species reported to cause human and animal diseases (Jain et al., 2011), including *Fusarium solani* (the most common), *F. anthophilum, F. oxysporum, F. proliferatum* and *F. verticoides*. These *Fusarium* species produce mycotoxins such as trichothecenes mainly nivalenol, deoxynivalenol (DON), T-2 and HT-2 toxins, zearalenone (ZEN), and fumonisins (B1, B2, and B3) (Antonissen et al., 2014).

As a global problem, mycotoxins are toxic fungal metabolites that can contaminate a wide array of food and feed (Al-Maqtoofi and Thornton, 2016). Fusarium mycotoxins are capable of inducing acute and chronic toxic effects and can be life-threatening. The toxic effects mainly depend on the type of mycotoxins, the level and duration of exposure, the animal species, and the age of the animal exposed (Al-Maqtoofi and Thornton, 2016). Intake of high doses of mycotoxin may lead to acute mycotoxicoses characterized by well-described clinical symptoms (Smith et al., 2005; Antonissen et al., 2014). Exposure of pigs to high concentrations of DON causes abdominal distress, malaise, diarrhea, emesis, and even shock or death. Fumonisins lead to pulmonary edema in pigs due to cardiac insufficiency, cause equine leukoencephalomalacia (ELEM), and target the brains of horses (Devreese et al., 2013).

Some secondary metabolites and nanoparticles (NPs) can be biosynthesized from microorganisms. Generally, NPs can play an important role in eliminating environmental stresses and microbial infections and can enhance growth and performance in farm animals (Alagawany et al., 2021a; Abdelnour et al., 2020a; Reda et al., 2020; Sheiha et al., 2020; Alagawany et al., 2021b). Turner and Butler (2014) demonstrated the critical role of NPs in treating invasive fungal infections, especially those caused by yeast fungi such as *Candida* species. The NPs showed unique characteristics due to their tremendously small size and high surface area to the volume ratio (Singh et al., 2011).

Selenium (Se) is an essential trace element present in humans, animals, and some microorganisms; and is considered a vital cofactor of anti-oxidant enzymes such as thioredoxin reductase and glutathione peroxidase (Husen and Siddiqi, 2014; Srivastava and Mukhopadhyay, 2015). The SeNPs have potential for use in nanomedicines for their antimicrobial and anticancer properties (Forootanfar et al., 2014; Wadhwani et al., 2016). By using the recent approaches of nanotechnology, the biological synthesis of SeNPs with high efficiency, low-cost and accurate productivity has replaced the traditional physical and chemical procedures (Wadhwani et al., 2016). Biosynthesis of NPs involves the use of uni- and multi-cellular microorganisms including bacteria and fungi (El-Saadony et al., 2018; El-Saadony et al., 2021a; El-Saadony et al., 2021b; El-Saadony et al., 2021c; El-Saadony et al., 2021d; Reda et al., 2021), yeasts (Moghaddam et al., 2017; Shamsuzzaman et al., 2017), algae (Azizi et al., 2014), and some nonliving viral particles (Nam et al., 2006).

There have been investigations for an economical and straightforward biological method for the biotransformation of SeNPs using lactic acid bacteria (LAB) (Radhika and Gayathri, 2015). Thus, the use of whole bacterial cells or bacterial enzymes is an excellent substitute for the large-scale commercial biotransformation of SeNPs. The toxic form of selenium in selenite can be converted into non-toxic Se (insoluble in water) by microorganisms (Radhika and Gayathri, 2015).

Long-term water or plant consumption from Se–rich soil may lead to skin injury and early hair loss. Consequently, efforts have been made to convert toxic Se compounds to beneficial non-toxic Se using bacteria (Bajaj et al., 2012). Microorganisms such as *Lactobacillus acidophilus, Lactobacillus casei, Lactobacillus helveticus, Lactobacillus rhamnosus, Lactobacillus plantarum, Klebsiella pneumoniae, Streptococcus thermophilus,* and *Bifidobacterium* can act as small nano-factories secreting enzymes converting metal ions to metal NPs (Sasidharan and Balakrishnaraja, 2014; Radhika and Gayathri, 2015; Alam et al., 2020).

Due to the limitless microorganisms that can biosynthesize Se, researchers have focused on detecting novel effective isolates. In medicine, SeNPs have been reported to show low toxicity and high biological activity (Hartikainen et al., 2000; Wang et al., 2007). In addition, many studies have shown that some organic forms of Se have anticarcinogenic characteristics (Tapiero et al., 2003).

Candida and *Fusarium* infections are difficult to cure and can be lethal to animals, so novel antimicrobial formulations are needed. Accordingly, the current work aimed to (i) synthesize SeNPs using LAB, (ii) study the optimum culture conditions required for the production of these biogenic SeNPs, and (iii) examine the potential of these LAB-SeNPs as antifungal agents against pathogenic fungi in animals.

2. Materials and methods

2.1. Collection of human breast milk samples

Breast milk samples were obtained from three healthy breast-feeding volunteers. Milk samples were aseptically collected in sterile containers using clean gloves. Nipples were first washed with soap and sterile water, and the first milk drops (~500 μl) were discarded. The collected samples were stored at 4 °C until transporting to the laboratories of the Agricultural Microbiology Department, Faculty of Agriculture, Zagazig University, Egypt, for immediate processing.

2.2. Isolation of LAB from human breast milk

A ten-fold dilution of each milk sample was prepared in 0.9% sterile saline solution. Each dilution (0.1 ml each) was spread across the surface of selective agar media in sterilized plastic petri dishes (90 mm diameter) using sterilized L-shaped spreaders. For each dilution, three plates were used for each sample.

For the isolation of *Lactobacillus* species, de Man Rogosa and Sharpe (MRS) agar medium (CM0361, Oxoid Ltd., Basingstoke, Hampshire, UK) at pH 6.5 was used. However, for the isolation of bifidobacteria, MRS agar amended with cysteine (Sigma–Aldrich Chemie GmbH, Taufkirchen, Germany) at pH 5.2 was used (Argyri et al., 2013).

The cultures were incubated using AnaeroGen sacks (Oxoid Ltd.) at 37 ± 2 °C in an anaerobic GasPak system (Becton Dickinson, NJ, USA) for 48 h. Colonies were randomly collected from each sample and purified using streak plate technique on MRS agar medium. All bacterial cultures were kept at a temperature of 4 °C until use.

2.3. Production of LAB-SeNPs

Luria-Bertani (LB) broth was prepared by dissolving 10 g tryptone, 5 g yeast extract, and 5 g sodium chloride in 1000 ml distilled water (pH 7.5). The enrichment medium used in the current study was prepared by dissolving 0.5 g sodium nitrate, 5 g sodium chlo-

ride, 0.1 g ammonium chloride, 2.7 g di-potassium hydrogen phosphate, 3 g tryptone, 1 g beef extract, 0.5 g yeast extract, and 3 g glucose in 1000 ml distilled water. LB medium and enrichment medium were as described by Radhika and Gayathri (2015). Freshly cultivated LAB isolates were inoculated into 100 ml LB broth and placed in a shaking incubator at 170 rpm until reaching log phase (~12 h) at 35 °C according to Radhika and Gayathri (2015) with some modifications. The supernatant was discarded after centrifugation at 6,000 × g for 10 min. The bacterial pellet for each LAB was homogenized in 100 ml of the enrichment medium supplemented with 4.0 mM of Na_2SeO_3 (Sigma–Aldrich) as described by Radhika and Gayathri (2015). The flasks were incubated in a shaking incubator at 170 rpm at 35 °C for 40 h. After incubation, the formed SeNPs were harvested by centrifugation at 8,000 × g for 10 min, and washed four times with distilled water. The LAB-SeNPs were further analyzed using multiple characterization techniques (Boroumand et al., 2019).

The LAB selection for further experiments was based on their ability to change the bright yellow medium to red color after a 32 h incubation. The presence of red color in the medium containing Na_2SeO_3 and the tested bacterium approves the transformation of Na_2SeO_3 to SeNPs by the LAB isolate. Only four LAB isolates were able to transform Na_2SeO_3 to red SeNPs. The superior LAB isolate (HM1) possessing the highest production of stable SeNPs was chosen for the biosynthesis of LAB-SeNPs for all the experiments described below. This isolate was the fastest to transform Na_2SeO_3 to SeNPs, and produced a dark red color by 32 h compared to the other three LAB isolates, which produced pale red color after 40 h of incubation.

2.4. Identification of the superior LAB isolate HM1

The selected isolate (HM1) was putatively identified according to its morphological, biochemical, and physiological characteristics as recommended by Bergey's Manual of Systematic Bacteriology (Logan and De vos, 2009). The tests included cell morphology, Gram reaction, production of catalase enzyme and ammonia (NH_3), the ability to grow at 15 °C (5 days) and 45 °C (2 days) in MRS broth, and salt tolerance (4%, and 6.5% NaCl in MRS). Sugar fermentation tests were also carried out using trehalose, lactose, raffinose, sucrose, cellobiose, galactose, xylose, mannitol, melezitose, melibiose, ribose, sorbitol, and arabinose (Logan and De vos, 2009).

The identification of isolate HM1 was confirmed by matrix-assisted laser desorption ionization-time of flight mass spectrometry (MALDI-TOF MS) (Nacef et al., 2017) in addition to the phylogenetic analysis using 16S rRNA gene alignment sequences.

DNA of the LAB isolate HM1 was extracted and purified (Sambrook et al., 1989). The amplification procedures were followed using PCR (Veriti 96 well thermal cycler, Applied Biosystems®, San Francisco, CA, USA) and the QIA quick PCR purification kit (Baek et al., 2010). The 16S rRNA gene was amplified using the set 27 forward primer (5′AGAGTTT GATCMTGGCTCAG-3′) and 1492 reverse primer (5′-TACGGYTACCTTGTTACG ACTT-3′), according to Srivastava et al. (2008). The gene was sequenced using a 3500 Genetic Analyzer (Applied Biosystems®), using a peak block ramp rate of 3.9 °C⁄sec, reaction volume range of 10–100 μl, sample ramp rate of ± 3.35 °C⁄sec, and a temperature range (metric): 4.0–99.9 °C.

The phylogenetic tree was constructed using the neighbor-joining method (Saitou and Nei, 1987). Trees replicate (%) which associated with taxa clustered was calculated with the bootstrap test (100 replicates) (Felsenstein, 1985). The evolutionary distances were computed using the maximum composite as Tamura et al. (2004) method and are in the units of the number of base substitutions per site. Evolutionary analyses were conducted using

Molecular Evolutionary Genetics Analysis Version X (MEGAX) software (Kumar et al., 2016).

2.5. Optimization of culture conditions to improve the production of LAB-SeNPs

Several experiments were carried out to determine the optimum culture conditions required to improve the production of LAB-SeNPs. The freshly prepared bacterial inoculum grown on enrichment medium was supplemented with Na_2SeO_3 under various growth conditions described below. The conditions tested were; pH values (5.0, 6.0, 7.0, 8.0, 9.0, and 10.0), temperature (20, 25, 30, 35, 40, and 45 °C), and different concentrations of Na_2SeO_3 (1, 2, 3, 4, 5, and 6 mM). The flasks were incubated at different time intervals (1, 8, 16, 24, 32, and 40 h) and agitated at 100, 120, 140, 160, 180, and 200 rpm using a shaking incubator. Optical density (OD) was measured at 300 nm (OD_{300}) using a scanning spectrophotometer (UV-2101/3101 PC; Shimadzu Corporation, Analytical Instruments Division, Kyoto, Japan). These experiments were carried out according to Ghorbani et al. (2011); Wadhwani et al. (2017); and El-Saadony et al. (2020a) with some modifications. In each of these experiments, all factors were kept constant except for one varied factor.

2.6. Separation and purification of LAB-SeNPs

The LAB-SeNPs were centrifuged at 8,000 × g for 10 min, and the pellet was re-suspended in sterile distilled water. The LAB-SeNPs were lyophilized by freeze-drying (Thermo Fisher Scientific, Waltham, MA, USA) at −60℃ for 24 h and kept at 4 °C until further use (Wadhwani et al., 2017). The stability of the LAB-SeNPs was confirmed after ten weeks of cold storage by the absence of precipitates.

2.7. Characterization of LAB-SeNPs

After observing LAB-SeNPs formation by the media changing color from yellow to dark red, they were further characterized by ultraviolet (UV)–visible spectroscopy. The prepared mixture was monitored using Laxco™ dual-beam spectrophotometer, alpha series, 200–1000 nm (Mettler-Toledo LLC., Columbus, OH, USA) (Forough and Farhadi, 2010) to detect the surface plasmon resonance (SPR) of the obtained absorbance peak for LAB-SeNPs.

Fourier-transform infrared spectroscopy (FTIR; Bruker Tensor, Kaller, Germany) analysis was performed (Chattopadhyay et al., 2013) to determine the interaction between proteins found in cell-free extract and LAB-SeNPs. The FTIR was also used to identify the potential active compounds in the bacterial cell-free extract.

The LAB-SeNPs were also exposed to energy-dispersive X-ray spectroscopy (EDX) using JEOL (JSM–IT200 Series, Peabody, MA, USA) in order the determine the elemental composition of LAB-SeNPs. The shape and size of LAB-SeNPs were measured using transmission electron microscopy (TEM; JEOL Ltd., Tokyo, Japan) (Mendez et al., 2011).

Dynamic light scattering (DLS) (Malvern Panalytical, Malvern, UK) measured the particle size of nanoparticles in dispersals and aggregation rate (Gunti et al., 2019). The polydispersity index (PDI) measures the NPs' homogeneous nature; the smaller the PDI, the more homogeneous NPs (Gunti et al., 2019).

The size distribution of LAB-SeNPs was monitored at 27 ± 2 °C using a Zetasizer nano range (Malvern Panalytical, Malvern, UK). The Zeta potential of the NPs was measured to determine its surface charge using a zeta-potential instrument (Malvern Panalytical, Malvern, UK) (Gunti et al., 2019).

The nature of LAB-SeNPs was further analyzed using X-ray diffraction (XRD). The LAB-SeNPs cast was collected on a glass slide

and observed under D8 Advance Brucker X-ray diffractometer with Cu Kα (1.54°A) (Brucker Corporation, Billerica, MA, USA) as described by Ganachari et al. (2012).

2.8. Preparation of chemically produced SeNPs (Che-SeNPs)

The SeNPs were fabricated using the wet chemical method (Shar et al., 2019). Briefly, 4 g of ascorbic acid was mixed in 20 ml sterilized deionized water on a magnetic stirrer for 10 min at 30C. A 0.01 mol solution of Na_2SeO_3 was dissolved in 200 ml sterilized deionized water and mixed at 90 °C for 1 h. Drops of ascorbic acid solution were slowly added to the Na_2SeO_3 solution for 10 min. The colorless Na_2SeO_3 gradually changed from yellow to red color, indicating that the Che-SeNPs were successfully fabricated. The mixture was then centrifuged at 7,500 × g for 10 min, and the pellet was removed by rinsing five times with sterilized deionized water. The che-SeNPs obtained were overnight vacuum-dried at 60 °C, and stored at 4 °C. All other factors were kept constant to reach the optimum conditions.

2.9. Determination of the antifungal activity of LAB-SeNPs

The antifungal activities of the LAB-SeNPs and Che-SeNPs were tested against the following fungal species: *Candida albicans* ATCC 4862, *C. glabrata* ATCC 64677, *C. krusei* ATCC 14243, *C. parapsilosis* ATCC 22019, *C. tropicalis* ATCC 66029, *Fusarium oxysporum* ATCC 62506, and *F. solani* ATCC 38341. The tested *Candida* and fungi were cultivated on Sabouraud's dextrose agar plates (SDA) (Lab M Ltd., Heywood, Lancashire, UK) and the plates were incubated at optimum condition for *Candida* and *Fusarium* (37 °C for 2 days and 30 °C for 5 days), respectively (Balouiri et al., 2016). The antifungal activities of LAB-SeNPs and che-SeNPs (15, 30, 45, 60, and 75 μg ml^{-1}) against these fungal species were evaluated using the agar disc diffusion assay (Hariharan et al., 2012). The tested *Candida* spp., were grown on SDB at 37C until concentration of approximately 10^5 CFU ml^{-1}. *Fusarium* spp., were grown on Sabouraud dextrose agar (SDA) medium for 5 days at 30C, and 6 mm mycelial discs were obtained (Saeed et al., 2017). *Candida* spp., inoculum (100 μl) was spread over SDA plates, and *Fusarium* mycelial discs were added in the center of SDA plates. The antifungal activity of LAB-SeNPs and Che-SeNPs levels (15, 30, 45, 60, and 75 μg ml^{-1}) was evaluated using the agar disc diffusion assay method (Hariharan et al., 2012). Discs (6 mm diam.) were saturated with each concentration of LAB-SeNPs, Che-SeNPs, and sodium selenite (Na_2SeO_3; control) then was put on the sides of seeded SDA plates, the plates were incubated at optimum condition for *Candida* and *Fusarium* (37 °C for 2 days and 30 °C for 5 days), respectively. The antifungal activity was estimated by measuring the inhibition zones diameters (mm). Three plates were used for each fungal isolate. The interaction between LAB-SeNPs and the *Fusarium* species was also observed by scanning electron microscopy (SEM) (JEOL, Ltd., Tokyo, Japan) (Bozzola and Russell, 1999).

2.10. Determination of the minimum inhibitory concentration and minimum fungicidal concentration of Che-SeNPs and LAB-SeNPs

The minimum inhibitory concentration (MIC) of Che-SeNPs and LAB-SeNPs was estimated by micro broth dilution method (Saeed et al., 2017; Ashour et al., 2020). Aliquots of 500 μl for each Che-SeNPs and LAB-SeNP concentration (15, 30, 45, 60, and 75 μg ml^{-1}) were added to tubes containing Sabouraud dextrose broth (SDB) (Lab M) inoculated with 500 μl of *Candida* or *Fusarium* inoculum ($\sim10^5$ CFU ml^{-1}). Tubes were incubated at optimum conditions for *Candida* and *Fusarium* (37 °C for 2 days and 30 °C for 5 days), respectively. The obtained turbidity was measured at 600 nm using

a spectrophotometer (Shimadzu Corporation). The lowest concentration of Che-SeNPs or LAB-SeNPs, which inhibited the fungal growth, was recorded as the MIC. In addition, the lowest concentration of Che-SeNPs or LAB-SeNPs which inhibited the fungal growth, was considered to be the minimum fungicidal concentration (MFC) (Abdelnour et al., 2020a; Ashour et al., 2020). The MFC was estimated by sub-culturing the MIC levels of Che-SeNPs or LAB-SeNPs onto sterile SDA plates. the plates were incubated at optimum condition for *Candida* and *Fusarium* (37 °C for 2 days and 30 °C for 5 days), respectively.

2.11. Statistical analysis

Probability analysis was performed (Finney, 1971). Parameters were analyzed using SPSS Version 20.0 for windows (SPSS Inc., Chicago, IL, USA). All tests were independently replicated three times. Data were subjected to analysis of variance (ANOVA), and Fisher's protected least significant difference (LSD) test at $P = 0.05$ was applied to compare significant differences among means for all analyses.

3. Results

3.1. Isolation of LAB from human breast milk

In the current study, 15 different LAB isolates were obtained from human breast milk on MRS, and MRS agar amended with cysteine, under anaerobic conditions. Ten different isolates were tentatively selected based on their cultural and morphological features. The ten isolates were purified on MRS agar.

3.2. Screening of LAB-SeNPs

The first step in the screening process involved testing the ten selected LAB for their ability to convert the color of the medium from bright yellow to red color at the end of the incubation period. The red color in the medium containing Na_2SeO_3 and the tested bacterium confirms the transformation of Na_2SeO_3 to SeNPs by the LAB isolates (Fig. 1). Out of the ten LAB isolates tested, only four (HM1, HM5, HM6, and HM7) could transform Na_2SeO_3 to SeNPs, and produced red color. The remaining six LAB isolates failed to produce any red color and were excluded in the remaining experiments. Only isolate HM1 was selected for the biosynthesis of LAB-SeNPs as it was the fastest isolate in transforming Na2SeO3 to SeNPs, and therefore it produced a dark red color by 32 h (Fig. 1). The other three isolates took 48 h and only produced pale red color.
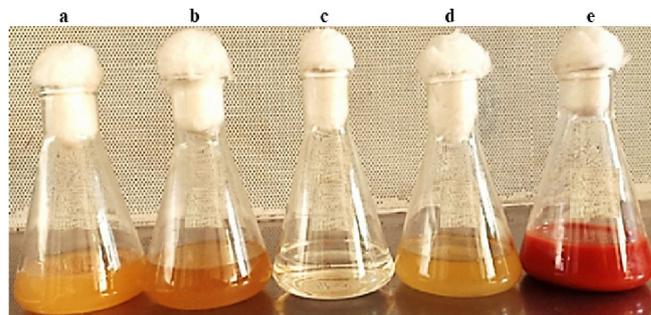

Fig. 1. |Production of selenium nanoparticles (SeNPs) by *Lactobacillus paracasei* HM1 (a) *Lactobacillus paracasei* HM1 in Luria-Bertani (LB) broth medium, (b) supernatant of *L. paracasei* HM1, (c) sodium selenite (Na_2SeO_3), (d) supernatant of *L. paracasei* HM1 with Na_2SeO_3 after 32 h of incubation at 35 °C, and (e) pellet of *L. paracasei* HM1 homogenized in enrichment medium supplemented with Na_2SeO_3 after 32 h of incubation at 35 °C. In (e), note the formation of dark red color in flask.

3.3. Identification of the superior LAB isolate HM1

The LAB Isolate HM1 was a Gram-positive, catalase-negative, and non-spore-forming bacterium. It did not produce NH_3 from arginine or gas from glucose, suggesting that this isolate is homo-fermentative. Isolate HM1 successfully grew at 15 °C, but not at 45 °C, and was tolerant to NaCl concentrations of 4 and 6.5%. The morphological, biochemical, and physiological characteristics of LAB Isolate HM1 is presented in Table 1. The identification of the LAB isolate HM1 was further confirmed using MALDI-TOF MS.

The 16S rRNA sequencing results (Fig. 2) matched the identification of the isolate using MALDI-TOF MS. The LAB isolate HM1 was highly similar to the 16S rRNA gene sequences of other *L. paracasei* showing a 98.5–100% sequence identity range. The 16S rRNA nucleotide sequence was deposited in GenBank with an accession number (MW390875) under *L. paracasei* strain HM1. In addition, a comparative phylogenetic tree was established to find the relationship between the identified strain and the existing *Lactobacillus* group based on the 16S rRNA gene sequences (Fig. 2). The phylogenic analysis revealed that the isolated strain HM1 belonged to the genus *Lactobacillus* and mainly to the phylogenetic clade of *L. paracasei*. The present data suggest that the LAB, *L. paracasei* HM1, is a promising bacterium for the production of SeNPs.

3.4. Optimization of the synthesis of SeNPs by L. paracasei HM1

The effects of different pH values of the culture medium on the production of SeNPs by *L. paracasei* HM1 are represented in Table 2. There was greater absorbance of the formed SeNPs at pH 6.0 compared to the other pH values. Above pH 6.0, the absorbance of LAB-SeNPs was significantly ($P < 0.05$) decreased. When fresh bacterial inoculum of *L. paracasei* HM1 was mixed with Na_2SeO_3, the absorbance measurements increased with increasing temperature (20 to
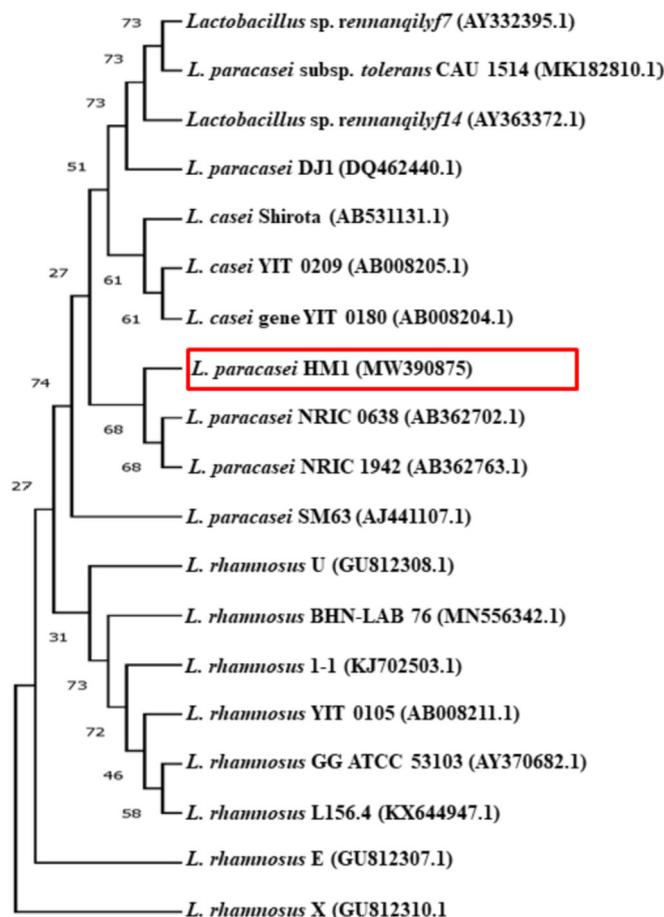

Fig. 2. Identification of *Lactobacillus paracasei* HM1 based on phylogenetic characteristics. Analysis of the phylogenetic tree of the 16S rRNA gene sequence of *L. paracasei* HM1 (MW 390875) with other *Lactobacillus* species.

Table 1
Morphological and biochemical characteristics of the selected lactic acid bacterium (LAB) isolate HM1.

Characteristics	LAB isolate HM1
Gram reaction	+
Endospore formation	–
Production of catalase	–
Production of NH_3 from arginine	–
Growth at	
15°C	+
45°C	–
4% NaCl	+
6.5% NaCl	+
Production of gas from glucose	–
Fermentation of	
Glucose	+
Lactose	+
Mannitol	+
Galactose	+
Cellobiose	+
Xylose	+
Sucrose	+
Ribose	+
Sorbitol	+
Melezitose	+
Raffinose	–
Xylose	–
Melibiose	–
Arabinose	–
Trehalose	–

+, growth or positive reaction; -, no growth or negative reaction.

35 °C), with a maximum value obtained at 35 °C (Table 2). We found that increasing the temperature above 35 °C significantly ($P < 0.05$) decreased the formation of *L. paracasei*-SeNPs and at further temperature increases led to the aggregation of NPs.

Biotransformation of SeNPs was detected at Na_2SeO_3 concentrations up to 6.0 mM (Table 2). The red color intensity was enhanced when Na_2SeO_3 concentration increased from 1.0 to 4.0 mM; indicating that 4.0 mM Na_2SeO_3 was considered to be optimal for the SeNPs synthesis (Table 2). It was also noted that concentrations of Na_2SeO_3 above 4.0 mM significantly ($P < 0.05$) decreased the formation of *L. paracasei*-SeNPs.

We also investigated the effect of incubation time (1, 8, 16, 24, 32, and 40 h) (Table 2). At incubations of<1 h, there was no production of SeNPs, which could be attributed to the reduction of Na_2SeO_3 redox potential. Moreover, there was an increase in the absorption peak as the reaction time increased (Table 2). Thus, more *L. paracasei*-SeNPs were produced by increasing the incubation period to 32 h, indicating that 32 h was the optimum incubation period to complete the reaction. It is noteworthy to mention that there was no significant ($P > 0.05$) difference between the 32 and 40 h incubation periods.

Another significant parameter that affects SeNPs output is the agitation level. We showed that SeNPs had an optimum production at 160 rpm during incubation compared to the other speeds (Table 2). Increasing the agitation speed from 100 to 160 rpm provided a more homogeneous environment, increasing the reaction's

Table 2
In vitro growth conditions affecting the reaction between *Lactobacillus paracasei* HM1 and sodium selenite (Na$_2$SeO$_3$).

pH values	5.0	6.0	7.0	8.0	9.0	10.0
	1.23 ± 0.001b	1.93 ± 0.003a	1.11 ± 0.001b	0.93 ± 0.007bc	0.63 ± 0.005c	0.32 ± 0.001d
Temperature (°C)	20	25	30	35	40	45
	0.93 ± 0.007c	1.12 ± 0.001c	1.75 ± 0.007b	2.12 ± 0.005a	1.89 ± 0.003ab	1.71 ± 0.009b
Na$_2$SeO$_3$ (mmol)	1	2	3	4	5	6
	1.42 ± 0.001d	1.62 ± 0.003c	1.82 ± 0.001bc	2.14 ± 0.007a	1.92 ± 0.009b	1.61 ± 0.007c
Reaction time (h)	1	8	16	24	32	40
	1.32 ± 0.003c	1.45 ± 0.001c	1.76 ± 0.007bc	1.89 ± 0.003b	2.12 ± 0.009a	2.11 ± 0.007a
Agitation speed (rpm)	100	120	140	160	180	200
	1.34 ± 0.009c	1.46 ± 0.003c	1.53 ± 0.007bc	2.17 ± 0.001a	1.96 ± 0.005ab	1.89 ± 0.001b

Optical density (OD) measurements at 300 nm (OD$_{300}$) were determined using spectrophotometer. Mean ± standard deviation ($n = 3$) of OD$_{300}$. Values with the same letter within a row are not significantly ($P > 0.05$) different according to Fisher's Protected LSD Test.

surface area. However, above 160 rpm there was significantly ($P < 0.05$) less formation of *L. paracasei*-SeNPs (Table 2).

In conclusion, the optimum cultivation conditions for *L. paracasei*-SeNPs were pH 6.0, 35℃, 4.0 mM Na$_2$SeO$_3$, 32 h reaction time, and 160 rpm agitation speed (Table 2).

3.5. Characterization of L. paracasei-SeNPs

3.5.1. Visualization of L. paracasei-SeNPs color

The reaction between Na2SeO3 and fresh inoculum of *L. paracasei* HM1 occurred rapidly and steadily in the enrichment media at 35 °C. The solution changed from light yellow to reddish-yellow after 2 h of incubation, gradually becoming dark red by 32 h, without further color change after that (Fig. 1). In the current study, SeNPs were formed inside the cells when *L. paracasei* HM1 pellets were added to enrichment medium supplemented with Na$_2$SeO$_3$. However, there was no change in the color when *L. paracasei* HM1 supernatant was added to Na$_2$SeO$_3$ (Fig. 1).

When UV–visible spectroscopy was used, the absorption peak for LAB-SeNPs was observed in the range of 200–1000 nm, and the absorbance of 300 nm was the peak for *L. paracasei* HM1 (Fig. 3A).

3.5.2. Determination of the shape and size of L. paracasei-SeNPs using TEM

Using TEM, the bio-fabrication of *L. paracasei* HM1 and the NPs size distribution were observed (Fig. 3B). The SeNPs size attained by the culture of *L. paracasei* HM1, under optimum conditions of 4.0 mM Na$_2$SeO$_3$ at pH 6.0 under 35 °C incubation for 32 h ranged between 3 and 50 nm in diameter. The TEM micrographs of the prepared *L. paracasei*-SeNPs showed that the *L. paracasei*-SeNPs were hexagonal monodispersed NPs (Fig. 3B). The *L. paracasei*-SeNPs did not aggregate, indicating the stabilization by the capping protein/peptide.

3.5.3. FTIR analysis

FTIR spectrum of *L. paracasei*-SeNPs showed nine distinct peaks at 3430.07, 2425.73, 1643.40, 1410.24, 1081.65, 988.34, 828.53, 608.68 and 542.80 cm^{-1} (Fig. 4). The current data indicated a strong, broad peak at 3430.07 cm^{-1}, corresponding to the presence of primary and secondary amines and amide linkages in the protein and alcohols/phenols, respectively. The peak of 2425.73 cm^{-1} indicated the functional groups of aromatics and alkynes. The bands appearing at 1643.40 and 1410.24 cm^{-1} were assigned for alkenes and aromatics, respectively (Fig. 4). The peak at 1081.65 cm^{-1} proved the presence of phenol and alcoholic
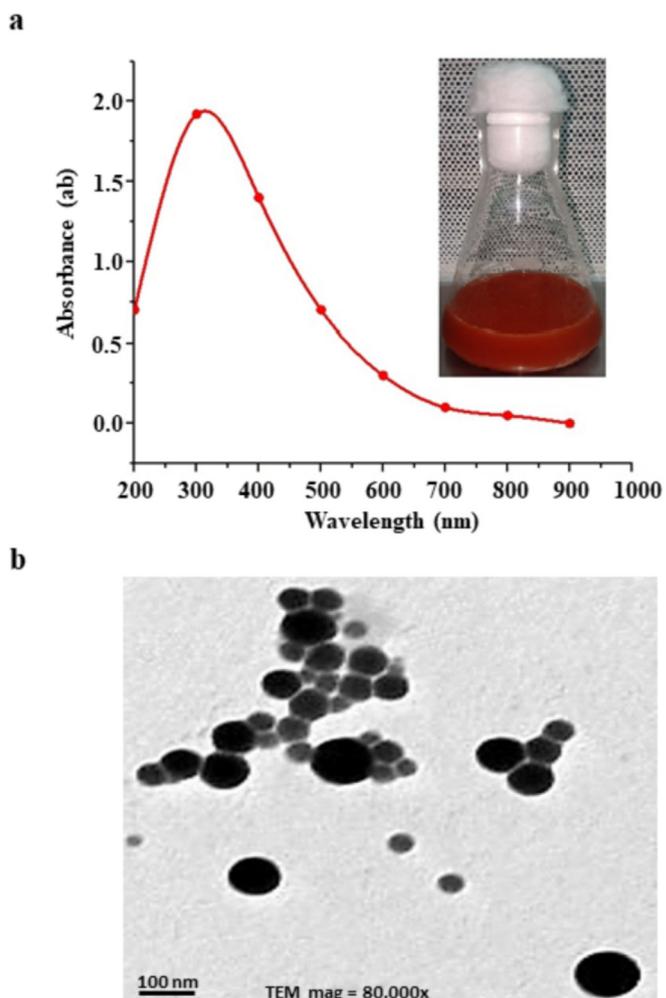
Fig. 3. Features of selenium nanoparticles (SeNPs) produced by *Lactobacillus paracasei* HM1. (a) Ultraviolet–visible spectroscopy spectrum of fabricated *L. paracasei*-SeNPs; and (b) transmission electron microscopy (80,000X) of SeNPs produced by *L. paracasei* HM1. In (a), note the formation of dark red color in the flask.

compounds. The peaks at 608.68, 988.34, and 828.53 cm^{-1} were due to the aromatic C–H bending. The peak at 542.80 cm^{-1} related to metal–carbon stretch (Fig. 4).
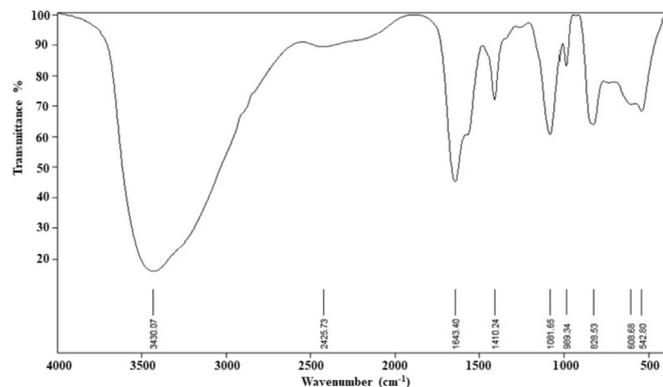
Fig. 4. Structural characteristics of selenium nanoparticles (SeNPs) produced by *Lactobacillus paracasei* HM1 using Fourier-transform infrared spectroscopy.

Fig. 6. Structural characteristics of selenium nanoparticles (SeNPs) produced by *Lactobacillus paracasei* HM1 using energy-dispersive X-ray spectroscopy.

3.5.4. XRD analysis

The XRD analysis was used to investigate the structural characteristics of the formed *L. paracasei*-SeNPs. The XRD patterns of the *L. paracasei*-SeNPs were analyzed to determine the peak intensity, width, and position (Fig. 5). The obtained results indicated that the structure of the *L. paracasei*-SeNPs was spherical, crystalline, and all had a similar diffraction profile. The XRD spectrum of LAB-SeNPs showed eight peaks at Braggs angles, confirming the Se phase (Fig. 5). These XRD peaks at 2θ of 28.61°, 31.19°, 40.01°, 45.02°, 56.21°, 66.23°, 75.11°, and 84.74° could return it to the 100, 101, 110, 102, 111, 201, 112 and 202 crystallographic planes of the spherical shape of Se crystals. Thus, the current results suggest that the biosynthesized SeNPs were well-crystallized.

3.5.5. EDX analysis

We assessed the EDX analysis of LAB-SeNPs. The Se peak was at 1.4 keV (Fig. 6), which indicates that the bio-SeNPs were pure Se.

3.5.6. DLS analysis

The DLS analysis measured the size distribution and polydispersity index (PDI) of *L. paracasei*-SeNPs. The average size of *L. paracasei*-SeNPs were 56.91 ± 1.8 nm (Fig. 7A), and the biotransformed *L. paracasei*-SeNPs were found to be monodispersed.

Zeta potential observed the surface charges gained by *L. paracasei*-SeNPs, which was responsible for the stability of the colloidal *L. paracasei*-SeNPs. Potential colloidal stability was predicted by the magnitude of zeta potential. *L. paracasei*-SeNPs zeta potential was found to be 20.1 ± 0.6 mV (Fig. 7B).
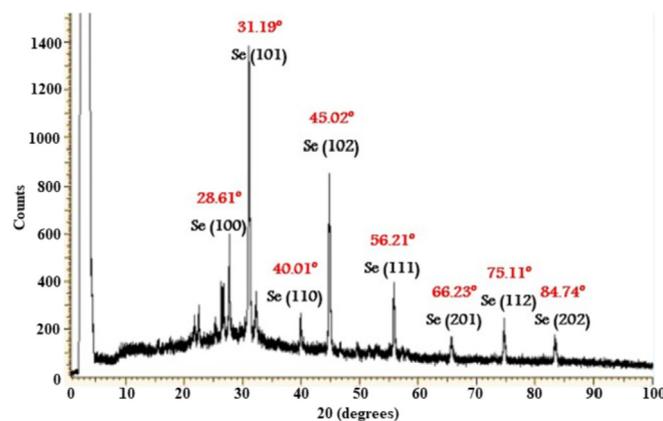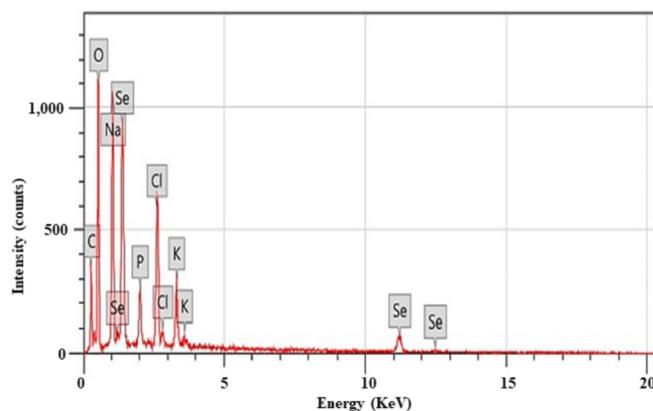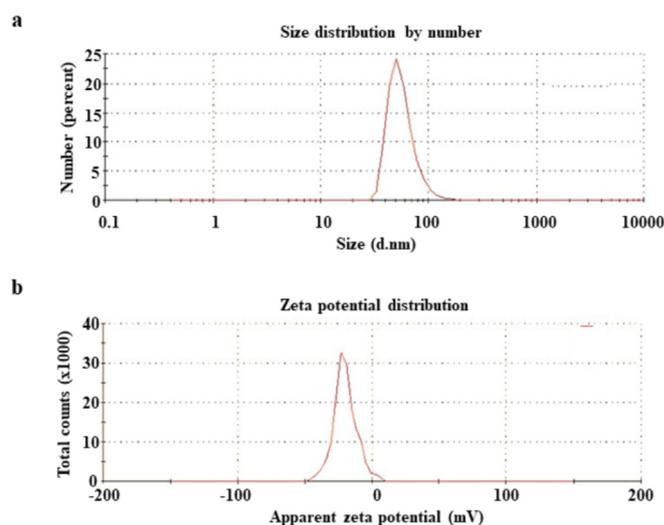

Fig. 7. Size and charge characterization of selenium nanoparticles (SeNPs) produced by *Lactobacillus paracasei* HM1. (a) Dynamic light scattering analysis of SeNPs showing size distribution of particles; and (b) zeta potential analysis showing the charge distribution on the SeNPs generated by *L. paracasei* HM1.

3.6. Determination of the antifungal activity of L. paracasei-SeNPs

The antifungal activity of Che-SeNPs and *L. paracasei*-SeNPs, in the present study, was evaluated against Candida spp., (*C. albicans*, *C. glabrata*, *C. krusei*, *C. parapsilosis* and *C. tropicalis*) and *Fusarium* spp., (*F. oxysporum* and *F. solani*) using the disc diffusion method. *In vitro* results showed the effective antifungal activity of Che-SeNPs and *L. paracasei*-SeNPs against the five *Candida* and two *Fusarium* spp. (Table 3).

The results also showed that the *in vitro* antifungal activity of LAB-SeNPs was more effective than Che-SeNPs against the tested *Candida* and *Fusarium* spp. (Table 3). The interaction of LAB-SeNPs and Che-SeNPs with *Candida* spp., is presented in Table 3.

The data revealed that increasing the concentrations of *L. paracasei*-SeNPs, significantly ($P < 0.05$) increased the diameter of the inhibition zone when different species of *Candida* were tested (Table 3; Fig. 8). *L. paracasei*-SeNPs displayed more efficient and significant antifungal activity than the Che-SeNPs (Table 3). In general, all fungal strains were affected by the Che-SeNPs and LAB-SeNPs at all levels used (15, 30, 45, 60, and 75 µg ml^{-1}) compared to 15 µg ml^{-1} Na$_2$SeO$_3$ (control) that gave an inhibition zone of<9 mm (Table 3; Fig. 8). All concentrations of LAB-SeNPs showed

Fig. 5. Structural characteristics of selenium nanoparticles (SeNPs) produced by *Lactobacillus paracasei* HM1 using X-ray diffraction.

Table 3
Antifungal activity demonstrated by inhibition zone (mm), minimum inhibitory concentration (µg ml⁻¹) and minimum fungicidal concentration (µg ml⁻¹) caused by the chemically produced selenium nanoparticles (Che-SeNPs) compared to selenium nanoparticles synthesized by *Lactobacillus paracasei* HM1 (LAB-SeNPs) at different concentrations against some pathogenic *Candida* and *Fusarium* species.

Fungal strains	Che-SeNPs Concentration (µg ml⁻¹)					LAB-SeNPs Concentration (µg ml⁻¹)					Che		LAB	
	15	30	45	60	75	15	30	45	60	75	MIC	MFC	MIC	MFC
C. albicans ATCC 4862	17 ± 0.2aD	19 ± 0.4aD	22 ± 0.3aC	25 ± 0.4aB	27 ± 0.2aAB	23 ± 0.2aC	25 ± 0.5aB	26 ± 0.2aB	27 ± 0.3aB	29 ± 0.1aA	55d	95de	55bc	100c
C. parapsilosis ATCC 22019	16 ± 0.3abE	18 ± 0.3abD	20 ± 0.1bD	22 ± 0.1bC	25 ± 0.6abB	22 ± 0.4aB	24 ± 0.2aB	25 ± 0.2aB	26 ± 0.4abAB	27 ± 0.5abA	65bc	120d	60b	105c
C. krusei ATCC 14243	13 ± 0.5cE	17 ± 0.3bD	19 ± 0.4bC	21 ± 0.5bB	24 ± 0.6bAB	19 ± 0.6bC	20 ± 0.3bC	22 ± 0.2bB	24 ± 0.5bAB	25 ± 0.3bA	75b	135bc	70a	120b
C. glabrata ATCC 64677	12 ± 0.4cdF	15 ± 0.2cE	17 ± 0.4cC	20 ± 0.1bcB	22 ± 0.5cAB	17 ± 0.8bcC	18 ± 0.4bcC	20 ± 0.4bcB	22 ± 0.8cAB	23 ± 0.4bcA	85a	150a	65ab	110bc
C. tropicalis ATCC 66029	13 ± 0.3cE	16 ± 0.5bcD	18 ± 0.5bcC	21 ± 0.4bB	23 ± 0.4cAB	18 ± 0.7bC	19 ± 0.2bC	21 ± 0.5bcB	23 ± 0.5bcAB	24 ± 0.5bcA	80ab	150a	70a	130a
F. oxysporum ATCC 62506	14 ± 0.5cF	17 ± 0.4bE	19 ± 0.3bD	22 ± 0.3bC	24 ± 0.5bB	16 ± 0.8cE	19 ± 0.3bD	22 ± 0.6bC	24 ± 0.5bB	26 ± 0.2abA	70b	130c	50c	90d
F. solani ATCC 38341	16 ± 0.6abF	19 ± 0.2aE	21 ± 0.5aDE	23 ± 0.3aD	26 ± 0.8abC	18 ± 0.7bE	22 ± 0.2abD	25 ± 0.5aC	27 ± 0.4aB	29 ± 0.3aA	60c	100de	45c	80de

MIC, minimum inhibitory concentration; MFC, minimum fungicidal concentration. Values are means of 3 independent replicates for each experiment (means ± SD). Values with the same lower or upper case letter within a column or a row, respectively, are not significantly (P > 0.05) different according to Fisher's Protected LSD Test.
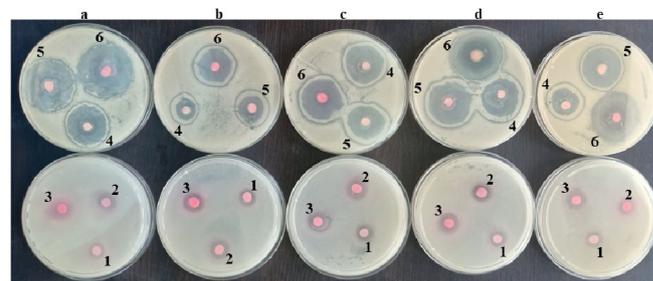

Fig. 8. Antifungal activity of selenium nanoparticles (SeNPs) synthesized by *Lactobacillus paracasei* HM1 on *Candida* species. (a) *C. albicans* ATCC 4862; (b) *C. glabrata* ATCC 64677; (c) *C. tropicalis* ATCC 66029; (d) *C. parapsilosis* ATCC 22019; and (e) *C. krusei* ATCC 14243. The concentration of SeNPs diffused into agar disc: (1) 15 µg chemically produced SeNPs/disc, (2) 15 µg *L. paracasei*-SeNPs/disc, (3) 30 µg *L. paracasei*-SeNPs/disc, (4) 45 µg *L. paracasei*-SeNPs/disc, (5) 60 µg *L. paracasei*-SeNPs/disc, and (6) 75 µg *L. paracasei*-SeNPs/disc.

significant ($P < 0.05$) increased diameters of inhibition zones when compared to the Che-SeNPs (Table 3). Generally, the inhibition zones increased as *L. paracasei*-SeNPs levels increased (Table 3), while the maximum LAB-SeNPs concentration produced a maximum inhibition zone of 29 mm with *F. solani* and *C. albicans* (Table 3).

Based on statistical analysis, all the antifungal activity of LAB-SeNPs levels significantly ($P < 0.05$) excelled the Che-SeNPs concentration with a relative increase of 20% against the animal pathogenic fungi species used in this study (Table 3).

In addition, SEM revealed that the *L. paracasei*-SeNPs severely damaged the *Fusarium* hyphae compared to the non-treated *Fusarium* (control) (Fig. 9).

3.7. Determination of the MIC and MFC of Che-SeNPs and LAB-SeNPs

C. albicans, *C. parapsilosis*, and the two *Fusaruim* spp. were the most sensitive species to the antifungal activity of Che-SeNPs and LAB-SeNPs (15–75 µg ml⁻¹) (Table 3). *C. albicans, C. parapsilosis,* F. oxysporum, and F. solani had MICs of 55, 60, 50, and 45 µg ml⁻¹, respectively. The MICs of the remaining *Candida* spp., significantly ($P < 0.05$) increased by 15–20% over *C. albicans, C. parapsilosis*; and 30–40% over *F. solani* and *F. oxysporum,* respectively (Table 3). The LAB-SeNPs MFC was in the range of 80–130 µg ml⁻¹, which ensured the complete killing of all tested fungi.

The same pattern was also found when Che-SeNPs were used. However, the MIC and MFC levels significantly ($P < 0.05$) increased by 15–20%. Simply, the MIC and MFC levels of Che-SeNPs were in the range between 55 and 85 µg ml⁻¹ and 95–150 µg ml⁻¹, respectively (Table 3).
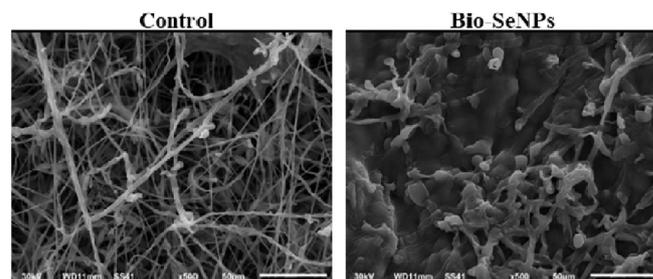

Fig. 9. Scanning electron micrograph (500X) showing the interaction between *Lactobacillus paracasei*-selenium nanoparticles (SeNPs) and *Fusarium oxysporum* ATCC 62506. Healthy *F. oxysporum* mycelium without *L. paracasei*-SeNPs (control; left panel), and damaged *F. oxysporum* mycelium with 75 µg ml⁻¹ *L. paracasei*-SeNPs (right panel).

4. Discussion

Fungal infection affects all living organisms in several ways, making them difficult to treat due to their resistance to common antifungal antibiotics and/or antifungal agents. *Fusarium* and *Candida* species infect animals as well as human; and in turn they cause several diseases. The aim of the current study was to create a green approach and low-cost technique for the biosynthesis of SeNPs using LAB to be used as antifungal agents. Biosynthesis of NPs involves the use of uni- and multi-cellular microorganisms (El-Saadony et al., 2021a–d).

In this respect, Olivares et al. (2006) have isolated four lactobacilli strains from human breast milk. They proposed that these lactobacilli strains could play an essential role in protecting neonates from various microbial infections and could be respectable in developing probiotic products for infants. It is well-known that breast milk constitutes of a non-stopping source of staphylococci, streptococci, bifidobacteria and LAB to infants' gut (Martín et al., 2009).

In the present study, the LAB isolate HM1 from human breast milk was found to be similar to *L. paracasei*. Neamtu et al. (2014) reported that seven LAB isolates obtained from human breast milk were identified as *L. paracasei* subsp. *paracasei* according to their ability to ferment 19 different sugars. The identification was also confirmed by MALDI-TOF MS, which is a rapid, accurate, and reliable technique and is generally used to identify bacterial isolates to the genus, species and subspecies levels (Duskova et al., 2012; Chalupová et al., 2014; Abdelnour et al., 2020b). Similar approaches have also been used to identify molds and yeasts (Bizzini et al., 2011). Furthermore, molecular techniques (e.g. 16S rRNA sequence analysis) have also confirmed the identification of the *Lactobacillus* strains to the species and subspecies levels (Wang et al., 2011; Verma and Mehata, 2016).

Xu et al. (2018) found that probiotic *Lactobacillus casei* 393 was able to transform the colorless, toxic form of Se, to reddish, non-toxic and elemental form. Eszenyi et al. (2011) have obtained conflicting results because they have used different probiotic species in the production of nano-sized 100–500 nm Se. Generally, to fabricate biological SeNPs by selected strains of lactobacilli, optimum conditions for biosynthesis must be provided. The medium pH influences the transformation of metal SeNPs by changing the form of biomolecules accountable for capping and stabilizing the NPs (Lortie et al., 1992). Temperature of 30°-37 °C is also a limiting factor, because the biomolecules-mediated sodium selenite reduction is active in this range (Singh et al., 2011; Saxena et al. 2016). Previously, it has been mentioned that high temperatures raise the kinetic energy, resulting in maximum NPs production and rapid synthesis rate (Shakibaie et al., 2011).

It was shown that the concentrations of Na_2SeO_3 between 1.0 and 4.0 mM did not affect the morphology of the final products (Shamsuzzaman et al., 2017); however, the concentration of 3.0 mM Na_2SeO_3 was considered to be ideal for synthesizing SeNPs by *Acinetobacter* sp. (Singh et al., 2011). It has been stated that the reduction rate of Se can be enhanced by increasing Se concentrations up to 19.0 mM (Lortie et al., 1992). However, the reduction rate may be reduced due to the toxicity of Se. Other researchers also reported that the red color intensity increases with time as the solutions were initially greyish-yellow and turned light red after 5 h of incubation (Shamsuzzaman et al., 2017).

It has been found that the time of reduction may vary from one species to another. For example, the color change has been observed by *L. rhamnosus* within 12 h, followed by *L. acidophilus* and *L. plantarum* after 18 h and 26 h of incubation, respectively (Radhika and Gayathri, 2015). In microbial cultivation, the aeration and dissolved oxygen are affected by the agitation speed (Yan et al.,

2005). The development of the dark red color demonstrated the formation of SeNPs (Azizi et al., 2014), which complies with the wavelength of the SPR of bio-SeNPs (Yan et al., 2005; Shakibaie et al., 2011; Saxena et al., 2016).

There are many studies associated with the formation of SeNPs that shows various absorption peaks, indicating the presence of SeNPs. In these studies, the peaks have appeared to be at 290 nm (Hemalatha et al., 2014), and the energetic absorption band has been located at 265 nm (Fesharaki et al., 2010). Moreover, another peak has been observed at 263 nm (Khiralla and El-Deeb, 2015). The UV–visible spectroscopy absorption spectra of SeNPs obtained from a culture broth have presented a distinctive property peak at 590 nm, resembling a large particle size of 183 ± 33 nm (Lin and Wang, 2005).

Previous studies have demonstrated that SeNPs can be synthesized by bacteria (Sasidharan and Balakrishnaraja, 2014); however, the main disadvantage was the production of large-sized SeNPs (Hnain et al., 2013). In the present study, SeNPs size particles ranged between 3 and 50 nm in diameter which was not in agreement with the other study (Hnain et al., 2013), which reported a size range of SeNPs between 100 and 550 nm, with a mean size of 245 nm (Neamtu et al., 2014). Similarly, *L. acidophilus* and *Bifidobacterium* sp. produced large SeNPs sizes of 50–500 nm and 400–500 nm, respectively; while *K. pneumoniae* has produced 200–300 nm SeNPs (Fesharaki et al., 2010). The recorded FTIR analysis suggested that organic molecules such as polyphenols, alkaloids, and terpenoids, as already reported (Kalainila et al., 2014), might surround the NPs. The peptides attached to NPs through carboxyl group residues have been reported (Balaji et al., 2009). Some studies have investigated that proteins can bind to NPs through cysteine or amine residues, indicating that these proteins may act as stabilizing agents (Mandal et al., 2005; El-Saadony et al., 2020a).

The recorded FTIR spectrum for the purified SeNPs powder and synthesized by *L. acidophilus* with bands at 3430 and 3417 cm^{-1} was attributed to the O-H stretching mode and the N-H stretch in amine groups, respectively (Shamsuzzaman et al., 2017). Broad peaks at 747, 783, and 791 cm^{-1} have been in accordance with C-H stretching motion, while a narrow peak at 1645 and 1651 cm^{-1} have been linked to C-C stretching (Shamsuzzaman et al., 2017). The carboxyl, amine and cysteine residues of peptides bind electrostatically with NPs. Hence, the proteins might coat the metal NPs to prevent the accumulation and stability in suspension (Lin and Wang, 2005). The amide linkages can give well-known signatures in the infrared region of the electromagnetic spectrum. The proteins with free amine groups or cysteine residues can bind to gold NPs (Gole et al., 2001).

The results coming from the current study indicated the presence of protein(s) in the supernatant aligned with previous findings (Raliya and Tarafdar, 2013). Overall, evidence of the existence of proteins in the supernatant is also supported by recent reports (El-Saadony et al., 2020a). Many researchers have stated that proteins can bind to SeNPs, either through free cysteine or amine groups in proteins (Raliya and Tarafdar, 2013; El-Saadony et al., 2020a). These proteins, existing over the SeNPs surface, may act as a capping agent for stabilization. Based on this spectrum fingerprint, it can be inferred that many functional groups are present and involved in the conversion of Se ions to SeNPs. Similar results with characterized SeNPs have previously been reported (Zhang et al., 2019).

Similar findings have also been demonstrated, where the obtained XRD patterns have shown the prominent peaks characteristic of the crystalline SeNPs at 2θ values of 23.5°, 29.7°, 41.4°, 43.7° and 45.4°; thus, corresponding to the crystal planes 100, 101, 110, 102 and 111, respectively (Fresneda et al., 2018). The average crys-

talline size of biogenic Se nanostructures, in the current study, measured by Scherrer's equation was about 34 nm. In another study by Singh et al. (2014), they have demonstrated a peak at 2θ value of 23.680, 29.788, and 43.9 of SeNPs produced by *Bacillus* sp., indicating the presence of Se which was reduced from selenite ions (Singh et al., 2014). This can be attributed to the different bioactive groups (e.g. polyphenols, alkaloids, carboxyl groups residues, and terpenoids) attached to the bio-SeNPs surface (Kalainila et al., 2014).

The peaks of oxygen (O), carbon (C), sodium (Na), phosphorus (P), chlorine (Cl), and potassium (K) may surround the NPs (Balaji et al., 2009). In the current study, other elements appeared alongside with SeNPs in EDX chromatogram may be due to the bacterial growth medium components. These results are in agreement with Wadhwani et al. (2017).

The NPs that have zeta potential values of > +30 mV or < − 30 mV (Ramya et al., 2015), maintained the stability of SeNPs as reported by Meléndrez et al. (2010). Electrostatic repulsion was generated between the NPs and that relied on the charges existing on the surface of NPs. The net negative charges on the surface of NPs inhibited aggregation and maintained stability. The bacterial protein covering the surface of the NPs has caused the negative charges responsible for stability (Dhanjal and Cameotra, 2010).

Here, the obtained LAB had powerful antifungal activities against animal pathogenic fungi especially, *Candida* and *Fusarium* species. Although *C. albicans* is considered the most virulent species of *Candida*, other species might be more pathogenic in certain animals, depending on the site of infection (Diekema et al., 2012). Cutaneous candidiasis is one of the most common skin diseases affecting dogs (Lewis, 2009). Oral and gastrointestinal mucosal candidiasis is common in birds, especially chickens (Odds, 1988; Maubon et al., 2014). Similar candidiasis have been observed in a number of animals (e.g. dogs and cats) at young ages (Odds, 1988). It has been reported that *C. guilliermondii* and *C. parapsilosis* cause miscarriages in horses and cattle, mastitis in dairy cows, calves, cats, dogs, horses, and rodents, as well as inflammation of the endocardial surface and eye inflammation in horses (Brito et al., 2009; Al-Yasiri et al., 2016). Candidiasis can also occur as a secondary bacterial infection. Thus, one should consider a feasible option *i.e.,* biogenic SeNPs, such as those produced by *L. paracasei* HM1 when the hosts do not respond to antibiotic treatments.

Fusarium spp., produces several mycotoxins, which in high doses can lead to severe mycotoxicoses. Where feed contaminated with these toxic mycotoxins has been administered, human consumption of animals, or their edible products, can cause severe brain damage or death (Pohlman and Chengappa, 2013). Feeding pigs on high levels of the mycotoxin DON leads to abdominal distress, malaise, diarrhea, vomiting, and even death (Pohlman and Chengappa, 2013). In horses, fumonisins can cause ELEM (Pitt, 1994). Combined exposure to low doses of DON, T-2 toxin, and ZEN reduces the number of goblet cells in pigs (Devreese et al., 2013). Administration of ZEN alone at higher doses increases goblet cell activity (Bouhet and Oswald, 2005).

The common antifungal drugs, including clotrimazole, econazole, miconazole, terbinafine, fluconazole, ketoconazole and amphotericin, are extreme irritants and can be lethal (Bossche et al., 2003). It has become necessary to develop new types of active, safe and cost-effective fungicidal materials. Biosynthesized SeNPs such as those reported by Shahverdi et al. (2010) and SeNPs produced by *L. paracasei* HM1in the current study could be safely used for that purpose.

The results, obtained in the current study, can be explained as being the succession of three mechanisms: 1) easy adhesion to cells, 2) penetration and consequently 3) damaging the cell structures (Guisbiers et al., 2017). It has been shown that SeNPs exhibit

high biological effects simultaneously with low toxicity levels (Meléndrez et al., 2010; Netala et al., 2016). Fluconazole, a potent antifungal drug, has shown vigorous antifungal activity against the tested species, and no inhibition zone in the control discs was recorded (Gudikandula and Maringanti, 2016; Netala et al., 2016; Rachitha et al., 2017).

There were some similarities in the action of *L. paracasei*-SeNPs on *F. oxysporum* when compared to the essential oil of *Mentha piperita* on *F. sporotrichioides* (Rachitha et al., 2017). It has been reported that the population of *F. sporotrichioides* was reduced by 90% when the fungal pathogen was treated with *M. piperita* essential oil at 1000 μg ml⁻¹. The effect of *M. piperita* essential oil on *F. sporotrichioides* was attributed to the DNA damage and cell wall disruption, which were the most common causes of cell death. The NPs were able to adhere to the cell wall and membrane due to electrostatic interactions; and therefore, disrupt the cell wall. This results in macromolecules' leakage or allows passage through the cell membrane to damage DNA, ultimately leading to cell death (Dakal et al., 2016; Anyasi et al., 2017; El-Saadony et al., 2020b).

The antimicrobial activity of SeNPs depends on the way they were synthesized. For instance, the antimicrobial efficacy of bio-SeNPs produced by *Bacillus mycoides* SelTE01 (Bio Se-NEMO-S) against *Staphylococcus aureus* ATCC 25923 and *Pseudomonas aeruginosa* NCTC 12934 at 6–24 h was more efficient than Che-SeNPs generated using ascorbic acid (Piacenza et al., 2017). In another study carried out by Sheiha et al. (2020), the bio-SeNPs (78 and 312 μg ml⁻¹) have shown the same antibacterial activity efficacy against all tested bacteria, while the Che-Se (2500 μg ml⁻¹) has shown moderate antimicrobial activity (Sheiha et al., 2020). The present results were consistent with a former study carried out by Cremonini et al. (2016) who demonstrated that Se produced by *B. mycoides* and *Stenotrophomonas maltophilia* exhibited stronger antimicrobial action than Che-SeNPs.

The chemical and physical production of NPs cannot be expanded to large-scale production due to several issues, including the presence of toxic organic solvents, hazardous intermediate compounds, and high-energy consumption. This might compromise the animal health and the environment due to the uncertainty in the composition of the final product. Therefore, the focus on using biological production methods is possibly safer for animal use (Keat et al., 2015; Gudikandula and Maringanti, 2016; El-Saadony et al., 2019). Bio-SeNPs and Se have similar biological activity in terms of antioxidant, antibacterial, and anticancer properties (Liu et al., 2004; Jayaprakash and Marshall, 2011; Turner and Butler, 2014; Wang et al., 2014). The NPs produced better activity against the biological materials, albeit the nanoscale sizes and large surface-to-volume ratio. Nano-Se has lower toxicity compared to other chemical forms of supplemented Se (Lippman et al., 2009; Kojouri et al., 2012). Synthesized SeNPs produced by *Bacillus* sp. have been used as an antifungal agent against *C. albicans,* with a MIC of 70 μg ml⁻¹ (Shakibaie et al., 2013).

The current study confirmed that the nanoscale biogenic SeNPs synthesized by *L. paracasei* HM1 had promising *in vitro* antifungal activity against the clinical fungal species of *Candida* and *Fusarium*. Yet, the mechanism of the antifungal effect against these animal pathogenic fungi is unknown and merits further *in vivo* studies. This will support the development of this class of antifungal "drug" to treat invasive candidiasis and mycotoxicosis in animals.

5. Conclusion

In this study, we investigated a novel treatment for potentially lethal infections in animals caused by *Candida* and *Fusarium* species. Biosynthesis of SeNPs using *L. paracasei* HM1 can be applicable at the commercial level to reduce the dependence on

traditional chemical production methods with harmful impacts on the animal health and environment. The SeNPs synthesized by *L. paracasei* HM1 showed better antifungal activity against the animal fungal pathogens tested in the current study compared to SeNPs synthesized by chemical methods. Biosynthesis of SeNPs using *L. paracasei* HM1 provides an eco-friendly and safe alternative with protective effects against the most damaging animal fungal pathogens.

Funding

Author contributions

M.T.E.-S, M.M.N., A.M.S., T.F.T., S.AQ, K.E.-T and A.S. conceived and designed the experiments. M.T.E.-S, M.M.N, A.M.S., T.F.T. and A.S. helped in conducting the experiment and collected literature. S.AQ. and K.E.-T helped in constructing the phylogenetic tree. M. T.E.-S, S.AQ., and K.E.-T. analyzed the data and drafted the manuscript. M.T.E.-S, M.M.N., A.M.S., T.F.T., A.S., A.N., N.Z., A.T., S.AQ, and K.E.-T. wrote and finally edited the manuscript. All the authors read and approved the final version of the manuscript.

Declaration of Competing Interest

The authors declare that they have no known competing financial interests or personal relationships that could have appeared to influence the work reported in this paper.

References

Abdelnour, S.A., El-Saadony, M.T., Saghir, S.A.M., Abd El-Hack, M.E., Al-shargi, O.Y.A., Al-Gabri, N., Salama, A., 2020a. Mitigating negative impacts of heat stress in growing rabbits via dietary prodigiosin supplementation. Livest Sci. 240, 104220. https://doi.org/10.1016/j.livsci.2020.104220.

Abdelnour, S.A., Swelum, A.A., Salama, A., Al-Ghadi, M.Q., Qattan, S.Y.A., Abd El-Hack, M.E., Khafaga, A.F., Alhimaidi, A.R., Almutairi, B.O., Ammari, A.A., El-Saadony, M.T., 2020b. The beneficial impacts of dietary phycocyanin supplementation on growing rabbits under high ambient temperature. Ital. J. Anim. Sci. 19, 1046–1056. https://doi.org/10.1080/1828051X.2020.1815598.

Alagawany, M., El-Saadony, M.T., Elnesr, S.S., Farahat, M., Attia, G., Madkour, M., Reda, F.M., 2021a. Use of lemongrass essential oil as a feed additive in quail's nutrition: its effect on growth, carcass, blood biochemistry, antioxidant and immunological indices, digestive enzymes and intestinal microbiota. Poult. Sci. 100, 101172. https://doi.org/10.1016/j.psj.2021.101172.

Alagawany, M., Madkour, M., El-Saadony, M.T., Reda, F.M., 2021b. *Paenibacillus polymyxa* (LM31) as a new feed additive: antioxidant and antimicrobial activity and its effects on growth, blood biochemistry, and intestinal bacterial populations of growing Japanese quail. Anim. Feed Sci. Technol. 276, 114920. https://doi.org/10.1016/j.anifeedsci.2021.114920.

Alam, H., Khatoon, N., Khan, M.A., Husain, S.A., Saravanan, M., Sardar, M., 2020. Synthesis of selenium nanoparticles using probiotic bacteria *Lactobacillus acidophilus* and their enhanced antimicrobial activity against resistant bacteria. J. Clust. Sci. 31, 1003–1011. https://doi.org/10.1007/s10876-019-01705-6.

Al-Maqtoofi, M., Thornton, C.R., 2016. Detection of human pathogenic *Fusarium* species in hospital and communal sink biofilms by using a highly specific monoclonal antibody. Environ. Microbiol. 18, 3620–3634. https://doi.org/10.1111/1462-2920.13233.

Al-Yasiri, M.H., Normand, A.C., Piarroux, R., Ranque, S., Mauffrey, J.F., 2016. Gut yeast communities in *Larus michahellis* from various breeding colonies. Med. Mycol. 55, 436–444. https://doi.org/10.1093/mmy/myw088.

Antonissen, G., Martel, A., Pasmans, F., Ducatelle, R., Verbruggke, E., Vandenbroucke, V., Li, S., Haesebrouck, F., van Immerseel, F., Croubels, S., 2014. The impact of *Fusarium* mycotoxins on human and animal host susceptibility to infectious diseases. Toxins. 6, 430–452. https://doi.org/10.3390/toxins6020430.

Anyasi, T.A., Jideani, A.I.O., Mchau, G.R.A., 2017. Effects of organic acid pretreatment on microstructure, functional and thermal properties of unripe banana flour. J. Food Meas. Charact. 11, 99–110. https://doi.org/10.1007/s11694-016-9376-2.

Argyri, A.A., Zoumpopoulou, G., Karatzas, K.A., Tsakalidou, E., Nychas, G.J., Panagou, E.Z., Tassou, C.C., 2013. Selection of potential probiotic lactic acid bacteria from fermented olives by *in vitro* tests. Food Microbiol. 33, 282–291. https://doi.org/10.1016/j.fm.2012.10.005.

Ashour, E.A., Abd El-Hack, M.E., Shafi, M.E., Alghamdi, W.Y., Taha, A.E., Swelum, A.A., Tufarelli, V., Mulla, Z.S., El-Ghareeb, W.R.R., El-Saadony, M.T., 2020. Impacts of green coffee powder supplementation on growth performance, carcass characteristics, blood indices, meat quality and gut microbial load in broilers. Agriculture. 10, 457. https://doi.org/10.3390/agriculture10100457.

Azizi, S., Ahmad, M.B., Namvar, F., Mohamad, R., 2014. Green biosynthesis and characterization of zinc oxide nanoparticles using brown marine macroalga *Sargassum muticum* aqueous extract. Mater. Lett. 116, 275–277. https://doi.org/10.1016/j.matlet.2013.11.038.

Baek, H., Ahn, H.R., Cho, Y.S., Oh, K.H., 2010. Antibacterial effects of *Lactococcus lactis* HK-9 isolated from feces of a newborn infant. Korean J. Microbiol. 46, 127–133.

Bajaj, M., Schmidt, S., Winter, J., 2012. Formation of Se nanoparticles by *Duganella* sp. and *Agrobacterium* sp. isolated from Se-laden soil of North-East Punjab, India. Microb. Cell Fact. 11, 64. https://doi.org/10.1186/1475-2859-11-64.

Balaji, D.S., Basavaraja, S., Deshpande, R., Mahesh, D.B., Prabhakar, B.K., Venkataraman, A., 2009. Extracellular biosynthesis of functionalized silver nanoparticles by strains of *Cladosporium cladosporioides* fungus. Colloids Surf B Biointerfaces. 68, 88–92. https://doi.org/10.1016/j.colsurfb.2008.09.022.

Balouiri, M., Sadiki, M., Ibnsouda, S.K., 2016. Methods for *in vitro* evaluating antimicrobial activity: a review. J. Pharm. Anal. 6, 71–79. https://doi.org/10.1016/j.jpha.2015.11.005.

Bizzini, A., Jaton, K., Romo, D., Bille, J., Prod'hom, G., Greub, G., 2011. Matrix-assisted laser desorption ionization-time of flight mass spectrometry as an alternative to 16S rRNA gene sequencing for identification of difficult-to-identify bacterial strains. J. Clin. Microbiol. 49, 693–696. https://doi.org/10.1128/JCM.01463-10.

Boroumand, S., Safari, M., Shaabani, E., Shirzad, M., Faridi-Majidi, R., 2019. Selenium nanoparticles: synthesis, characterization and study of their cytotoxicity, antioxidant and antibacterial activity. Matter. Res. Express. 6, 0850d8. https://doi.org/10.1088/2053-1591/ab2558.

Bossche, H.V., Engelen, M., Rochette, F., 2003. Antifungal agents of use in animal health–chemical, biochemical and pharmacological aspects. J. Vet. Pharmacol. Ther. 26, 5–29. https://doi.org/10.1046/j.1365-2885.2003.00456.x.

Bouhet, S., Oswald, I.P., 2005. The effects of mycotoxins, fungal food contaminants, on the intestinal epithelial cell-derived innate immune response. Vet. Immunol. Immunopathol. 108, 199–209. https://doi.org/10.1016/j.vetimm.2005.08.010.

Bozzola, J.J., Russell, L.D., 1999. Electron Microscopy: Principles and Techniques for Biologists. Jones and Bartlett, Boston, p. 670.

Brito, E.H.S., Fontenelle, R.O.S., Brilhante, R.S.N., Cordeiro, R.A., Monteiro, A.J., Sidrim, J.J.C., Rocha, M.F.G., 2009. The anatomical distribution and antimicrobial susceptibility of yeast species isolated from healthy dogs. Vet. J. 182, 320–326. https://doi.org/10.1016/j.tvjl.2008.07.001.

Chalupová, J., Raus, M., Sedlářová, M., Šebela, M., 2014. Identification of fungal microorganisms by MALDI-TOF mass spectrometry. Biotechnol. Adv. 32, 230–241. https://doi.org/10.1016/j.biotechadv.2013.11.002.

Chattopadhyay, S., Dash, S.K., Ghosh, T., Das, D., Pramanik, P., Roy, S., 2013. Surface modification of cobalt oxide nanoparticles using phosphonomethyl iminodiacetic acid followed by folic acid: a biocompatible vehicle for targeted anticancer drug delivery. Cancer Nano. 4, 103–116. https://doi.org/10.1007/s12645-013-0042-7.

Cremonini, E., Zonaro, E., Donini, M., Lampis, S., Boaretti, M., Dusi, S., Melotti, P., Lleo, M.M., Vallini, G., 2016. Biogenic selenium nanoparticles: characterization, antimicrobial activity and effects on human dendritic cells and fibroblasts. Microb. Biotechnol. 9, 758–771. https://doi.org/10.1111/1751-7915.12374.

Dakal, T.C., Kumar, A., Majumdar, R.S., Yadav, V., 2016. Mechanism basic of antimicrobial action of silver nanoparticles. Front. Microbiol. 7, 1831. https://doi.org/10.3389/fmicb.2016.01831.

Devreese, M., de Backer, P., Croubels, S., 2013. Overview of the most important mycotoxins for the pig and poultry husbandry. Vlaams Diergeneeskd. Tijdschr. 82, 171–180. https://doi.org/10.21825/vdt.v82i4.16694.

Dhanjal, S., Cameotra, S., 2010. Aerobic biogenesis of selenium nanospheres by *Bacillus cereus* isolated from coalmine soil. Microb. Cell Fact. 9, 52. https://doi.org/10.1186/1475-2859-9-52.

Diekema, D., Arbefeville, S., Boyken, L., Kroeger, J., Pfaller, M., 2012. The changing epidemiology of healthcare-associated candidemia over three decades. Diagn. Microbiol. Infect. Dis. 73, 45–48. https://doi.org/10.1016/j.diagmicrobio.2012.02.001.

Dušková, M., Šedo, O., Kšicová, K., Zdráhal, Z., Karpíšková, R., 2012. Identification of lactobacilli isolated from food by genotypic methods and MALDI-TOF MS. Int. J. Food Microbiol. 159, 107–114. https://doi.org/10.1016/j.ijfoodmicro.2012.07.029.

Dworecka-Kaszak, B., Biegańska, M.J., Dąbrowska, I., 2020. Occurrence of various pathogenic and opportunistic fungi in skin diseases of domestic animals: a retrospective study. BMC Vet. Res. 16, 248. https://doi.org/10.1186/s12917-020-02460-x.

El-Saadony, M.T., El-Hack, M.E.A., Taha, A.E., Fouda, M.M.G., Ajarem, J.S., Maodaa, S. N., Allam, A.A., Elshaer, N., 2020a. Ecofriendly synthesis and insecticidal application of copper nanoparticles against the storage pest *Tribolium castaneum*. Nanomaterials. 10, 587. https://doi.org/10.3390/nano10030587.

El-Saadony, M.T., Alkhatib, F.M., Alzahrani, S.O., Shafi, M.E., Abdel-Hamid, S.E., Taha, T.F., Aboelenin, S.M., Soliman, M.M., Ahmed, N.H., 2021c. Impact of mycogenic zinc nanoparticles on performance, behavior, immune response, and microbial load in *Oreochromis niloticus*. Saudi J. Biol. Sci. 28, 4592–4604. https://doi.org/10.1016/j.sjbs.2021.04.066.

El-Saadony, M.T., Desoky, E.S.M., Saad, A.M., Eid, R.S., Selem, E., Elrys, A.S., 2021d. Biological silicon nanoparticles improve *Phaseolus vulgaris* L. yield and minimize its contaminant contents on a heavy metals-contaminated saline soil. J. Environ. Sci. 106, 1–14. https://doi.org/10.1016/j.jes.2021.01.012.

El-Saadony, M.T., El-Wafai, N.A., El-Fattah, H.I.A., Mahgoub, S.A., 2018. Biosynthesis, optimization and characterization of silver nanoparticles biosynthesized by *Bacillus subtilis* ssp *spizienii* MT5 isolated from heavy metals polluted soil. Zagazig J. Agric. Res. 45, 2439–2454. https://doi.org/10.21608/zjar.2018.47889.

El-Saadony, M.T., El-Wafai, N.A., El-Fattah, H.I.A., Mahgoub, S.A., 2019. Biosynthesis, optimization and characterization of silver nanoparticles using a soil isolate of *Bacillus pseudomycoides* MT32 and their antifungal activity against some pathogenic fungi. Adv. Anim. Vet Sci. 7, 238–249. https://doi.org/10.17582/journal.aavs/2019/7.4.238.249.

El-Saadony, M.T., Sitohy, M.Z., Ramadan, M.F., Saad, A.M., 2021a. Green nanotechnology for preserving and enriching yogurt with biologically available iron (II). Innov. Food Sci. Emerg. Technol. 69, 102645. https://doi.org/10.1016/j.ifset.2021.102645.

El-Saadony, M.T., Saad, A.M., Najjar, A.A., Alzahrani, S.O., Shafi, M.E., Alkhatib, F.M., Selem, E., Desoky, E.-S., Fouda, S.E.E., El-Tahan, A.M., Hassan, M.A.A., 2021b. The use of biological selenium nanoparticles to suppress *Triticum aestivum* L. crown and root rot diseases induced by *Fusarium* species and improve yield under drought and heat stress. Saudi J. Biol. Sci. 28, 4461–4471. https://doi.org/10.1016/j.sjbs.2021.04.043.

Eszenyi, P., Sztrik, A., Babka, B., Prokisch, J., 2011. Elemental, nano-sized (100–500 nm) selenium production by probiotic lactic acid bacteria. Int. J. Biosci. Biochem. Bioinform. 1, 148–152. https://doi.org/10.7763/IJBBB.2011.V1.27.

Felsenstein, J., 1985. Confidence limits on phylogenies: a justification. Evolution. 39, 783–791. https://doi.org/10.2307/2408678.

Fesharaki, P.J., Nazari, P., Shakibaie, M., Rezaie, S., Banoee, M., Abdollahi, M., Shaverdi, R., 2010. Biosynthesis of selenium nanoparticles using *Klebsiella pneumoniae* and their recovery by a simple sterilization process. Braz. J. Microbiol. 41, 461–466. https://doi.org/10.1590/S1517-83822010000200028.

Finney, D.J., 1971. Probit Analysis. Cambridge University Press, New York. J. Pharm. Sci. 60, 1432–1432. https://doi.org/10.1002/jps.2600600940.

Fisher, M.C., Henk, D.A., Briggs, C.J., Brownstein, J.S., Madoff, L.C., McCraw, S.L., Gurr, S.J., 2012. Emerging fungal threats to animal, plant and ecosystem health. Nature 484 (7393), 186–194.

Forootanfar, H., Zare, B., Fasihi-Bam, H., Amirpour-Rostami, S., Ameri, A., Shakibaie, M., Nami, M.T., 2014. Biosynthesis and characterization of selenium nanoparticles produced by terrestrial actinomycete *Streptomyces microflavus* strain FSHJ31. Res. Rev. J. Microbiol. Biotechnol. 3, 47–53.

Forough, M., Farhadi, K., 2010. Biological and green synthesis of silver nanoparticles. Turkish J. Eng. Env. Sci. 34, 281–287. https://doi.org/10.3906/muh-1005-30.

Fresneda, M.A.R., Martín, J.D., Bolívar, J.G., Cantos, F.M.V., Bosch-Estévez, G., Moreno, M.F.M., Merroun, M.L., 2018. Green synthesis and biotransformation of amorphous Se nanospheres to trigonal 1D Se nanostructures: impact on Se mobility within the concept of radioactive waste disposal. Environ. Sci. Nano. 5, 2103–2116.

Ganachari, S.V., Bhat, R., Deshpande, R., Venkataraman, A., 2012. Extracellular biosynthesis of silver nanoparticles using fungi *Penicillium diversum* and their antimicrobial activity studies. BioNanoSci. 2, 316–321. https://doi.org/10.1007/s12668-012-0046-5.

Ghorbani, H., Attar, H., Safekordi, A.A., Sorkhabadi, S.M.R., 2011. Optimization of silver nanoparticles production by *E. coli* bacterium (DH5 alpha) and the study of reaction kinetics. Asian J. Chem. 23, 5111–5118.

Gole, A., Dash, C., Ramachandran, V., Sainkar, S.R., Mandale, A.B., Rao, M., Sastry, M., 2001. Pepsin-gold colloid conjugates: preparation, characterization, and enzymatic activity. Langmuir. 17, 1674–1679. https://doi.org/10.1021/la001164w.

Gudikandula, K., Maringanti, S.C., 2016. Synthesis of silver nanoparticles by chemical and biological methods and their antimicrobial properties. J. Exp. Nanosci. 11, 714–721.

Guisbiers, G., Lara, H.H., Mendoza-Cruz, R., Naranjo, G., Vincent, B.A., Peralta, X.G., Nash, K.L., 2017. Inhibition of *Candida albicans* biofilm by pure selenium nanoparticles synthesized by pulsed laser ablation in liquids. Nanomedicine. 13, 1095–1103.

Gunti, L., Dass, R.S., Kalagatur, N.K., 2019. Phytofabrication of selenium nanoparticles from *Emblica officinalis* fruit extract and exploring its biopotential applications: antioxidant, antimicrobial, and biocompatibility. Front. Microbiol. 30, 931. https://doi.org/10.3389/fmicb.2019.00931.

Hariharan, H., Al-Dhabi, N.A., Karuppiah, P., Rajaram, S.K., 2012. Microbial synthesis of selenium nanocomposite using *Saccharomyces cerevisiae* and its antimicrobial activity. Chalcogenide Lett. 9, 509–515.

Hartikainen, H., Xue, T., Piironen, V., 2000. Selenium as an anti-oxidant and pro-oxidant in ryegrass. Plant Soil. 225, 193–200. https://doi.org/10.1023/A:1026512921026.

Hemalatha, T., Krithiga, G., Kumar, B.S., Sastry, T.P., 2014. Preparation and characterization of hydroxyapatite-coated selenium nanoparticles and their interaction with osteosarcoma (SaOS-2) cells. Acta. Metall. Sin. (Engl. Lett.). 27, 1152-1158. Https://doi.org/10.1007/s40195-014-0153-0.

Hnain, A., Brooks, J., Lefebvre, D.D., 2013. The synthesis of elemental selenium particles by *Synechococcus leopoliensis*. Appl. Microbiol. Biotechnol. 97, 10511–10519.

Husen, A., Siddiqi, K.S., 2014. Plants and microbes assisted selenium nanoparticles: characterization and application. J. Nanobiotechnology. 12, 28. https://doi.org/10.1186/s12951-014-0028-6.

Jain, P.K., Gupta, V.K., Misra, A.K., Gaur, R., Bajpai, V., Issar, S., 2011. Current status of *Fusarium* infection in human and animal. Asian. J. Anim. Vet. Adv. 6, 201–227.

Jayaprakash, V., Marshall, J.R., 2011. Selenium and other antioxidants for chemoprevention of gastrointestinal cancers. Best Pract. Res. Clin. Gastroentrol. 25, 507–518.

Kalainila, P., Subha, V., Ravindran, R.S.E., Renganathan, S., 2014. Synthesis and characterization of silver nanoparticle from *Erythrina indica*. Asian. J. Pharm. Clin. Res. 7, 39–43.

Keat, C.L., Aziz, A., Eid, A.M., Elmarzugi, N.A., 2015. Biosynthesis of nanoparticles and silver nanoparticles. Bioresour. Bioprocess. 2, 47. https://doi.org/10.1186/s40643-015-0076-2.

Khiralla, G.M., El-Deeb, B.A., 2015. Antimicrobial and antibiofilm effects of selenium nanoparticles on some foodborne pathogens. LWT-Food Sci. Technol. 63, 1001–1007.

Kojouri, G.A., Jahanabadi, S., Shakibaie, M., Ahadi, A.M., Shahverdi, A.R., 2012. Effect of selenium supplementation with sodium selenite and selenium nanoparticles on iron homeostasis and transferrin gene expression in sheep: a preliminary study. Res. Vet. Sci. 93, 275–278.

Kumar, S., Stecher, G., Tamura, K., 2016. MEGA7: molecular evolutionary genetics analysis version 7.0 for bigger datasets. Mol. Biol. Evol. 33, 1870–1974. https://doi.org/10.1093/molbev/msw054.

Lewis, R.E., 2009. Overview of the changing epidemiology of candidemia. Curr. Med. Res. Opin. 25, 1732–1740. https://doi.org/10.1185/03007990902990817.

Lin, Z.-H., Wang, C.R.C., 2005. Evidence on the size-dependent absorption spectral evolution of selenium nanoparticles. Mater. Chem. Phys. 92, 591–594.

Lippman, S.M., Klein, E.A., Goodman, P.J., Lucia, M.S., Thompson, I.M., Ford, L.G., Parnes, H.L., Minasian, L.M., Gaziano, J.M., Hartline, J.A., Parsons, J.K., Bearden, J. D., Crawford, E.D., Goodman, G.E., Claudio, J., Winquist, E., Cook, E.D., Karp, D.D., Walther, P., Lieber, M.M., Kristal, A.R., Darke, A.K., Arnold, K.B., Ganz, P.A., Santella, R.M., Albanes, D., Taylor, P.R., Probstfield, J.L., Jagpal, T.J., Crowley, J.J., Meyskens, F.L., Baker, L.H., Coltman, C.A., 2009. Effect of selenium and vitamin E on risk of prostate cancer and other cancers: the selenium and vitamin E cancer prevention trial. JAMA. 301, 39. https://doi.org/10.1001/jama.2008.864.

Liu, M.Z., Zhang, S.Y., Shen, Y.H., Zhang, M.L., 2004. Selenium nanoparticles prepared from reverse micro-emulsion process. Chin. Chem. Lett. 15, 1249–1252.

Logan, N.A., De Vos, P., 2009. Genus I. Bacillus Cohn 1872, 174AL. In : De Vos, P., Garrity, G.M., Jones, D., Krieg, N.R., Ludwig, W., Rainey, F.A., Schleifer, K.H., Whitman, W.B., Eds., Bergey's Manual of Systematic Bacteriology, 2nd Edition, Springer, New York, 3, 21-128.

Lortie, L., Gould, W.D., Rajan, S., McCready, R.G.L., Cheng, K.-J., 1992. Reduction of selenate and selenite to elemental selenium by a *Pseudomonas stutzeri* isolate. Appl. Environ. Microbiol. 58, 4042–4044.

Mandal, S., Phadtare, S., Sastry, M., 2005. Interfacing biology with nanoparticles. Curr. Appl. Phys. 5, 118–127.

Martín, R., Jiménez, E., Heilig, H., Fernández, L., Marín, M.L., Zoetendal, E.G., Rodríguez, J.M., 2009. Isolation of bifidobacteria from breast milk and assessment of the bifidobacterial population by PCR-denaturing gradient gel electrophoresis and quantitative real-time PCR. Appl. Environ. Microbiol. 75, 965–969.

Maubon, D., Garnaud, C., Calandra, T., Sanglard, D., Cornet, M., 2014. Resistance of *Candida* spp. to antifungal drugs in the ICU: where are we now? Intensive Care Med. 40, 1241–1255.

Meléndrez, M.F., Cárdenas, G., Arbiol, J., 2010. Synthesis and characterization of gallium colloidal nanoparticles. J. Colloid. Interface Sci. 346, 279–287.

Mendez, M.A.A., Martínez, E.S.M., Arroyo, L.O., Portillo, G.C., Espindola, E.S., 2011. Synthesis and characterization of silver nanoparticles: effect on phytopathogen *Colletotrichum gloeosporioides*. J. Nanopart. Res. 13, 2525–2532. https://doi.org/10.1007/s11051-010-0145-6.

Moghaddam, A.B., Moniri, M., Azizi, S., Rahim, R.A., Ariff, A.B., Saad, W.Z., Namvar, F., Navaderi, M., Mohamad, R., 2017. Biosynthesis of ZnO nanoparticles by a new *Pichia kudriavzevii* yeast strain and evaluation of their antimicrobial and antioxidant activities. Molecules. 22, 872. https://doi.org/10.3390/molecules22060872.

Nacef, M., Chevalier, M., Chollet, S., Drider, D., Flahaut, C., 2017. MALDI-TOF mass spectrometry for the identification of lactic acid bacteria isolated from a French cheese: the Maroilles. Int. J. Food Microbiol. 247, 2–8. https://doi.org/10.1016/j.ijfoodmicro.2016.07.005.

Nam, K.T., Kim, D.W., Yoo, P.J., Chiang, C.Y., Meethong, N., Hammond, P.T., Chiang, Y. M., Belcher, A.M., 2006. Virus-enabled synthesis and assembly of nanowires for lithium-ion battery electrodes. Science. 312, 885–888. https://doi.org/10.1126/science.1122716.

Neamtu, B., Ovidiu, T., Neamtu, M., Mihaela, T., Mirela, H., Ionela, M., 2014. Identification of probiotic strains from human milk in breastfed infants with respiratory infections. Acta Univ. Cibiniensis. Ser. E: Food Technol. 18, 73–84. https://doi.org/10.2478/aucft-2014-0016.

Netala, V.R., Kotakadi, V.S., Domdi, L., Gaddam, S.A., Bobbu, P., Venkata, S.K., Ghosh, S.B., Tartte, V., 2016. Biogenic silver nanoparticles: efficient and effective antifungal agents. Appl. Nanosci. 6, 475–484.

Odds, F.C., 1988. Candida and Candidosis. a review and bibliography. 2nd ed. Baillière Tindall London, UK. 468pp.

Olivares, M., Diaz-Ropero, M.P., Martin, R., Rodriguez, J.M., Xaus, J., 2006. Antimicrobial potential of four *Lactobacillus* strains isolated from breast milk. J. Appl. Microbiol. 101, 72–79. https://doi.org/10.1111/j.1365-2672.2006.02981.x.

Piacenza, E., Presentato, A., Zonaro, E., Lemire, J.A., Demeter, M., Vallini, G., Tuner, R.J., Lampis, S., 2017. Antimicrobial activity of biogenically produced spherical Se-nanomaterials embedded in organic material against *Pseudomonas aeruginosa* and *Staphylococcus aureus* strains on hydroxyapatite-coated surfaces. Microb. Biotechnol. 10, 804–818. https://doi.org/10.1111/1751-7915.12700.

Pitt, J.I., 1994. The current role of *Aspergillus* and *Penicillium* in human and animal health. J. Med. Vet. Mycol. 32 (s1), 17–32. https://doi.org/10.1080/02681219480000701.

Pohlman, L.M., Chengappa, M.M., 2013. Yeasts—Cryptococcus, Malassezia, and Candida, in: McVey, S., Kennedy, M., Chengappa, M.M (Eds.), Veterinary Microbiology. Wiley-Blackwell, pp. 313–320.

Rachitha, P., Krupashree, K., Jayashree, G.V., Gopalan, N., Khanum, F., 2017. Growth inhibition and morphological alteration of *Fusarium sporotrichioides* by *Mentha piperita* essential oil. Pharmacognosy Res. 9, 74–79. https://doi.org/10.4103/0974-8490.199771.

Radhika, S.R.R., Gayathri, S., 2015. Extracellular biosynthesis of selenium nanoparticles using some species of *Lactobacillus*. Indian J. Geomarine. Sci. 43, 766–775.

Raliya, R., Tarafdar, J.C., 2013. ZnO nanoparticle biosynthesis and its effect on phosphorous-mobilizing enzyme secretion and gum contents in Clusterbean (*Cyamopsis tetragonoloba* L.). Agric. Res. 2, 48–57. https://doi.org/10.1007/s40003-012-0049-z.

Ramya, S., Shanmugasundaram, T., Balagurunathan, R., 2015. Biomedical potential of actinobacterially synthesized selenium nanoparticles with special reference to anti-biofilm, anti-oxidant, wound healing, cytotoxic and anti-viral activities. J. Trace Elem. Med. Biol. 32, 30–39. https://doi.org/10.1016/j.jtemb.2015.05.005.

Reda, F.M., El-Saadony, M.T., Elnesr, S.S., Alagawany, M., Tufarelli, V., 2020. Effect of dietary supplementation of biological curcumin nanoparticles on growth and carcass traits, antioxidant status, immunity and caecal microbiota of Japanese quails. Animals. 10, 754. https://doi.org/10.3390/ani10050754.

Reda, F.M., El-Saadony, M.T., El-Rayes, T.K., Attia, A.I., El-Sayed, S.A., Ahmed, S.Y., Madkour, M., Alagawany, M., 2021. Use of biological nano zinc as a feed additive in quail nutrition: biosynthesis, antimicrobial activity and its effect on growth, feed utilization, blood metabolites and intestinal microbiota. Ital. J. Anim. Sci. 20, 324–335. https://doi.org/10.1080/1828051X.2021.1886001.

Saeed, E.E., Sham, A., Salmin, Z., Abdelmowla, Y., Iratni, R., El-Tarabily, K., AbuQamar, S., 2017. *Streptomyces globosus* UAE1, a potential effective biocontrol agent for black scorch disease in date palm plantations. Front. Microbiol. 8, 1455. https://doi.org/10.3389/fmicb.2017.01455.

Saitou, N., Nei, M., 1987. The neighbor-joining method: a new method for reconstructing phylogenetic trees. Mol. Biol. Evol. 4, 406–425. https://doi.org/10.1093/oxfordjournals.molbev.a040454.

Sambrook, J., Fritsch, E.F., Maniatis, T., 1989. Molecular Cloning: A Laboratory Manual. Cold Spring Harbor Laboratory Press, Cold Spring Harbor, NY, p. 1546.

Sasidharan, S., Balakrishnaraja, R., 2014. Comparison studies on the synthesis of selenium nanoparticles by various microorganisms. Int. J. Pure App. Biosci. 2, 112–117.

Saxena, J., Sharma, P.K., Sharma, M.M., Singh, A., 2016. Process optimization for green synthesis of silver nanoparticles by *Sclerotinia sclerotiorum* MTCC 8785 and evaluation of its antibacterial properties. SpringerPlus. 5, 861. https://doi.org/10.1186/s40064-016-2558-x.

Seyedmousavi, S., Bosco, S.M.G., de Hoog, S., Ebel, F., Elad, D., Gomes, R.R., Jacobsen, I.D., Jensen, H.E., Martel, A., Mignon, B., Pasmans, F., Piecková, E., Rodrigues, A.M., Singh, K., Vicente, V.A., Wibbelt, G., Wiederhold, N.P., Guillot, J., 2018. Fungal infections in animals: a patchwork of different situations. Med. Mycol. 56, S165–S187. https://doi.org/10.1093/mmy/myx104.

Shahverdi, A.R., Fakhimi, A., Mosavat, G., Jafari-Fesharaki, P., Rezaie, S., Rezayat, S.M., 2010. Antifungal activity of biogenic selenium nanoparticles. World Appl. Sci. J. 10, 918–922.

Shakibaie, M., Forootanfar, H., Golkari, Y., Mohammadi-Khorsand, T., Shakibaie, M.R., 2011. Antibiofilm activity of biogenic selenium nanoparticles and selenium dioxide against clinical isolates of *Staphylococcus aureus*, *Pseudomonas aeruginosa*, and *Proteus mirabilis*. J. Trace Elem. Med. Biol. 29, 235–241. https://doi.org/10.1016/j.jtemb.2014.07.020.

Shakibaie, M., Shahverdi, A.R., Faramarzi, M.A., Hassanzadeh, G.R., Rahimi, H.R., Sabzevari, O., 2013. Acute and subacute toxicity of novel biogenic selenium nanoparticles in mice. Pharm. Biol. 51, 58–63. https://doi.org/10.3109/13880209.2012.710241.

Shamsuzzaman, Mashrai, A., Khanam, H., Aljawfi, R.N., 2017. Biological synthesis of ZnO nanoparticles using *C. albicans* and studying their catalytic performance in the synthesis of steroidal pyrazolines. Arab. J. Chem. 10, S1530–S1536. https://doi.org/10.1016/j.arabjc.2013.05.004.

Shar, A.H., Lakhan, M.N., Wang, J., Ahmed, M., Alali, K.T., Ahmed, R., Ali, I., Dayo, A.Q., 2019. Facile synthesis and characterization of selenium nanoparticles by the hydrothermal approach. Dig. J. Nanomater. Biostruct. 14, 867–872.

Sheiha, A.M., Abdelnour, S.A., Abd El-Hack, M.E., Khafaga, A.F., Metwally, K.A., Ajarem, J.S., Maodaa, S.N., Allam, A.A., El-Saadony, M.T., 2020. Effects of dietary biological or chemical-synthesized nano-selenium supplementation on growing rabbits exposed to thermal stress. Animals. 10, 430. https://doi.org/10.3390/ani10030430.

Singh, N., Saha, P., Rajkumar, K., Abraham, J., 2014. Biosynthesis of silver and selenium nanoparticles by *Bacillus* sp. JAPSK2 and evaluation of antimicrobial activity. Der. Pharm. Lett. 6, 175–181.

Singh, R.P., Shukla, V.K., Yadav, R.S., Sharma, P.K., Singh, P.K., Pandey, A.C., 2011. Biological approach of zinc oxide nanoparticles formation and its characterization. Adv. Mater. Lett. 2, 313–317. https://doi.org/10.5185/amlett.indias.204.

Smith, T.K., Diaz, G., Swamy, H., Diaz, D., 2005. Current concepts in mycotoxicoses in swine. In: Diaz, D. (Ed.), The Mycotoxin Blue Book. Nottingham University Press, Nottingham, pp. 235–248.

Srivastava, N., Mukhopadhyay, M., 2015. Biosynthesis and structural characterization of selenium nanoparticles using *Gliocladium roseum*. J. Clust. Sci. 26, 1473–1482. https://doi.org/10.1007/s10876-014-0833-y.

Srivastava, S., Singh, V., Kumar, V., Verma, P.C., Srivastava, R., Basu, V., Gupta, V., Rawat, A.K., 2008. Identification of regulatory elements in 16S rRNA gene of *Acinetobacter* species isolated from water sample. Bioinformation. 3, 173–176. https://doi.org/10.6026/97320630003173.

Tamura, K., Nei, M., Kumar, S., 2004. Prospects for inferring very large phylogenies by using the neighbor-joining method. Proc. Natl. Acad. Sci. U. S. A. 101, 11030–11035. https://doi.org/10.1073/pnas.0404206101.

Tapiero, H., Townsend, D.M., Tew, K.D., 2003. The antioxidant role of selenium and seleno-compounds. Biomed. Pharmacother. 57, 134–144. https://doi.org/10.1016/S0753-3322(03)00035-0.

Turner, S.A., Butler, G., 2014. The *Candida* pathogenic species complex. Cold Spring Harb. Perspect. Med. 2, 1–17 https://doi.org/10.1101/cshperspect.a019778.

Verma, A., Mehata, M.S., 2016. Controllable synthesis of silver nanoparticles using neem leaves and their antimicrobial activity. J. Radiat. Res. Appl. Sci. 9, 109–115. https://doi.org/10.1016/j.jrras.2015.11.001.

Wadhwani, S.A., Gorain, M., Banerjee, P., Shedbalkar, U.U., Singh, R., Kundu, G.C., Chopade, B.A., 2017. Green synthesis of selenium nanoparticles using *Acinetobacter* sp. sW30: optimization, characterization, and its anticancer activity in breast cancer cells. Int. J. Nanomed. 12, 6841–6855. https://doi.org/10.2147/IJN.S139212.

Wadhwani, S.A., Shedbalkar, U.U., Singh, R., Chopade, B.A., 2016. Biogenic selenium nanoparticles: current status and future prospects. Appl. Microbiol. Biotechnol. 100, 2555–2566. https://doi.org/10.1007/s00253-016-7300-7.

Wang, H., Zhang, J., Yu, H., 2007. Elemental selenium at nano size possesses lower toxicity without compromising the fundamental effect on selenoenzymes: comparison with selenomethionine in mice. Free Radic. Biol. Med. 42, 1524–1533. https://doi.org/10.1016/j.freeradbiomed.2007.02.013.

Wang, X., Sun, K., Tan, Y., Wu, S., Zhang, J., 2014. Efficacy and safety of selenium nanoparticles administered intraperitoneally for the prevention of growth of cancer cells in the peritoneal cavity. Free Radic. Biol. Med. 72, 1–10. https://doi.org/10.1016/j.freeradbiomed.2014.04.003.

Wang, Y., Chen, C., Ai, L., Zhou, F., Zhou, Z., Wang, L., Zhang, H., Chen, W., Guo, B., 2011. Complete genome sequence of the probiotic *Lactobacillus plantarum* ST-III. J. Bacteriol. 193, 313–314. https://doi.org/10.1128/JB.01159-10.

Xu, J., Li, Y., Yang, Z., Li, C., Liang, H., Wu, Z., Pu, W., 2018. Yeast probiotics shape the gut microbiome and improve the health of early-weaned piglets. Front. Microbiol. 9, 2011. https://doi.org/10.3389/fmicb.2018.02011.

Yan, G., Du, G., Li, Y., Chen, J., Zhong, J., 2005. Enhancement of microbial transglutaminase production by *Streptoverticillium mobaraense*: application of a two-stage agitation speed control strategy. Process Biochem. 40, 963–968. https://doi.org/10.1016/j.procbio.2004.04.002.

Yapar, N., 2014. Epidemiology and risk factors for invasive candidiasis. Ther. Clin. Risk Manag. 10, 95–105. https://doi.org/10.2147/TCRM.S40160.

Zhang, H., Zhou, H., Bai, J., Li, Y., Yang, J., Ma, Q., Qu, Y., 2019. Biosynthesis of selenium nanoparticles mediated by fungus *Mariannaea* sp. HJ and their characterization. Colloids Surf. A. Physicochem. Eng. Asp. 571, 9–16. https://doi.org/10.1016/j.colsurfa.2019.02.070.